Correspondence to: Professor Paul J. Low
Department of Chemistry
Durham University
South Rd, Durham, DH1 3LE UK
Email p.j.low@durham.ac.uk

The synthesis, molecular and electronic structure of cyanovinylidene complexes

Ella M. Long, Neil J. Brown, Wing Y. Man, Mark A. Fox, Dmitry S. Yufit, Judith A.K. Howard, and Paul J. Low*

Department of Chemistry, Durham University, South Rd, Durham, DH1 3LE, UK

Email p.j.low@durham.ac.uk, tel +44 (0)191 334 2114, fax +44 (0)191 384 4737

Abstract

Reaction of the readily available metal acetylide complexes Ru(C≡CC_6H_4R-4)$(PPh_3)_2$Cp (R = OMe, Me, H, CN, CO_2Me), Ru(C≡CFc)$(PPh_3)_2$Cp and Fe(C≡CC_6H_4R-4)(dppe)Cp (R = Me, H) with 1-cyano-4-dimethylaminopyridinium tetrafluoroborate affords cyanovinylidene complexes [Ru{C=C(CN)C_6H_4R-4}$(PPh_3)_2$Cp]BF_4, [Ru{C=C(CN)Fc}$(PPh_3)_2$Cp]BF_4 and [Fe{C=C(CN)C_6H_4R-4}(dppe)Cp]BF_4 in an experimentally simple fashion. These synthetic studies are augmented by refinements to the preparation of the key iron reagents FeCl(dppe)Cp and Fe(C≡CC_6H_4R-4)(dppe)Cp. Molecular structure determinations, electrochemical measurements, representative IR spectroelectrochemical studies and DFT studies have been used to provide insight into the electronic structure of the cyanovinylidene ligand, and demonstrate that despite the presence of the cyano-substituted methylidene fragment, reduction takes place on the vinylidene C_α carbon.

Keywords: vinylidene, ruthenium, iron, spectroelectrochemistry, molecular structure.

1. Introduction

Within the vast array of hydrocarbyl ligands that have been stabilised through coordination to metal centres, vinylidene $C{=}CH_2$ and other substituted examples of this prototypical unsaturated carbene occupy an important position, featuring prominantly from a historical perspective in the development of the discipline of organometallic chemistry [1 - 3], to applications as key intermediates in modern synthetic chemistry [4 - 6]. The first organometallic vinylidene complex, $Fe_2(\mu\text{-}\eta^1\text{-}C{=}CPh_2)(CO)_8$, was reported in 1966 and featured the diphenylvinylidene moiety in a $\mu\text{-}\eta^1$- bridging mode formed from the photolysis of $Fe(CO)_5$ with diphenylketene [7, 8]. The preparation of both *cis*- and *trans*-$[Fe_2\{\mu\text{-}\eta^1\text{-}C{=}C(CN)_2\}(\mu\text{-}CO)(CO)_2Cp_2]$, containing the $\mu\text{-}\eta^1$-dicyanovinylidene ligand, followed in 1972 [9] while the first monometallic vinylidene complexes, which also featured dicyanovinylidene ligands, were reported in that same year [10]. In the decades that have followed, the chemistry of vinylidene complexes, and other unsaturated carbenes such as allenylidene ($:C{=}C{=}CH_2$) [2, 11] and butatrienylidene ($:C{=}C{=}C{=}CH_2$) [12, 13] was extensively explored. The practical applications of the metal chemistry of vinylidenes and other unsaturated carbenes are well-established, and vividly illustrated by the use of these species in the development of catalysts for olefin metathesis and other organic transformations [14, 15]. Somewhat surprisingly, despite this significant interest in the general area of vinylidene ligand chemistry, the proliferation of complexes featuring different combinations of metal, supporting ligands and substituents on the vinylidene moiety, and the presence of cyanovinylidene ligands in the earliest reports

of this class of ligand, cyanovinylidene chemistry has remained largely unexplored [16], likely due to the less than convenient methods of preparation known to date.

The first preparations of dicyanovinylidene ligand complexes were based on nucleophilic substitution reactions between $Cl_2C=C(CN)_2$ and metal carbonyl anions. In the case of reactions between $[Fe(CO)Cp]^-$ and $Cl_2C=C(CN)_2$, the bimetallic complexes *cis*- and *trans*-$[Fe_2\{\mu_2\text{-}\eta^1\text{-}C=C(CN)_2\}(\mu\text{-}CO)(CO)_2Cp_2]$ were isolated in low (<3%) yield (Scheme 1) [9, 17], the *cis* isomer later being crystallographically characterised [18]. Reaction of $[Fe_2(\mu\text{-}CO)(\mu\text{-}CSMe)(CO)_2Cp_2]^+$ with the carbon nucleophile $[CH(CN)_2]^-$ provides and alternative, and higher yielding (53%), route to mixtures of *cis* and *trans*-$[Fe_2\{\mu_2\text{-}\eta^1\text{-}C=C(CN)_2\}(\mu\text{-}CO)(CO)_2Cp_2]$ (Scheme 1) [19].

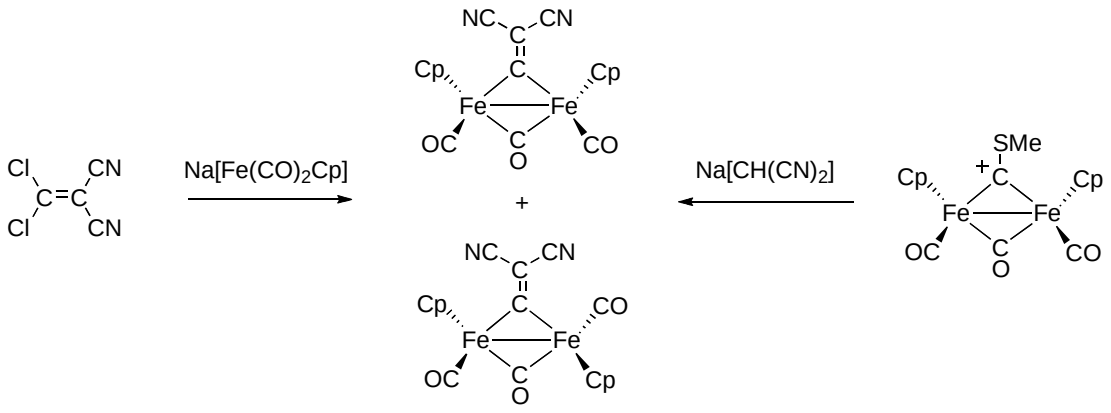

Scheme 1 The synthesis of *cis*- and *trans*-$Fe_2\{\mu\text{-}C=C(CN)_2\}(\mu\text{-}CO)(CO)_2Cp_2$ [17, 19].

The Group 6 metal carbonyl anions $[M(CO)_3Cp]^-$ (M = Mo, W) reacted smoothly with $Cl_2C=C(CN)_2$ to give 1-chloro-2,2-dicyanovinyl derivatives $[M\{C(Cl)=C(CN)_2\}(CO)_3Cp]$ in moderate yield [9, 17]. Subsequent thermolysis of the vinyl compounds in the presence of trivalent phosphorus ligands resulted in

carbonyl substitution and chloride migration to give a mixture of the *cis*- and *trans*-dicyanovinylidene complexes $MCl\{C=C(CN)_2\}(PR_3)_2Cp$ [20 - 22]; reactions of $Mo\{CCl=C(CN)_2\}(CO)_3Cp$ with Bu^tNC gave only the carbonyl substitution product $Mo\{CCl=C(CN)_2\}(CO)_2(CNBu^t)Cp$, the chlorovinyl ligand remaining unchanged (Scheme 2) [23].

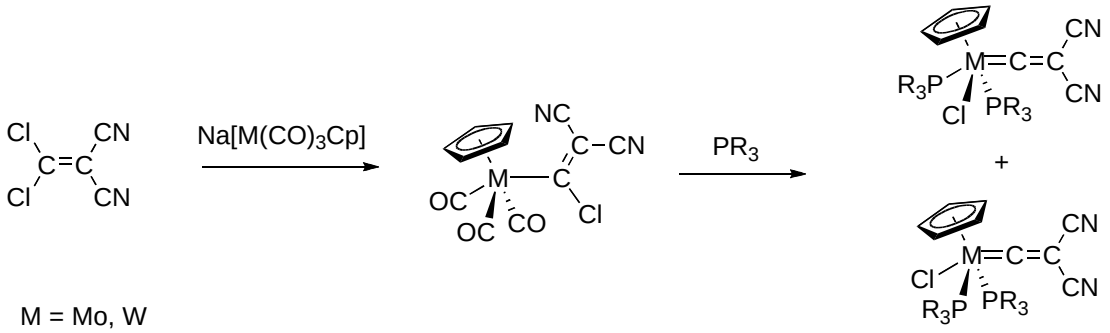

Scheme 2 The preparation of the terminal cyanovinylidene complexes $MCl\{C=C(CN)_2\}(PR_3)_2Cp$ (M = Mo, W) [9, 17, 20-22].

A series of anionic mono- and di-cyanovinylidene compounds has also been obtained following chloride displacement from $M(\equiv CCl)(CO)_2Tp^*$ [Tp* = hydridotris(3,5-dimethylpyrazol-1-yl)borate] by $Na[CHX_2]$ [X_2 = $(CN)_2$ (M = Mo, W); X_2 = $(CN)(CO_2Et)$ (M = Mo)] [24]. These anionic compounds can be represented by two limiting resonance forms, **A** and **B** (Scheme 3), the significance of form **A** being evidenced by the formation of simple adducts at C_β, whilst protonation or oxidation afford cyclic products.

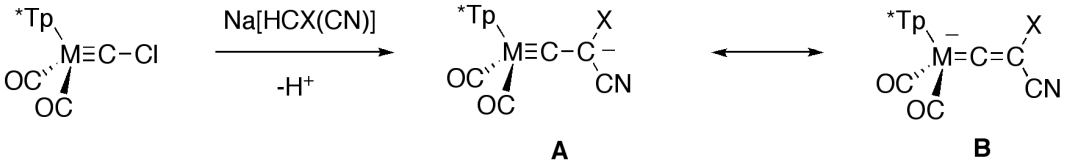

M = Mo, W; X = CO_2Et, CN
Tp* = hydridotris(3,5-dimethylpyrazol-1-yl)borate

Scheme 3 The formation of mono and dicyanovinylidenes from chloride displacement from M(≡CCl)$(CO)_2$Tp* [24].

In seeking to develop more expeditious routes to cyanovinylidene complexes, it is worth noting that half-sandwich ruthenium acetylide complexes such as Ru(C≡CPh)$(PPh_3)_2$Cp (**1**) react with a variety of electrophilic reagents [25, 26] including H^+ [27], alkyl halides [28], trialkyloxonium salts [29], diazonium salts and carbon-based electrophiles [30], including the masked example $B(C_6F_5)_3$ [31] halogens (Cl_2, Br_2, I_2) [32, 33], and cyanogen bromide, which acts as a halogen transfer agent [34], to form air-stable vinylidene complexes $[Ru\{=C=C(E)Ph\}(PPh_3)_2Cp]^+$. Indeed, whilst many synthetic routes to vinylidene complexes are known, the re-arrangement of a terminal alkyne or addition of an electrophile to the C_β carbon of a metal acetylide are perhaps the most general methods [1]. Nevertheless, recent reports of the rearrangement of *internal* alkynes in the presence of group 8 metal centres [35], including MCl(dppe)Cp in the presence of $NaBAr^F_4$ (M = Fe, Ru; Ar^F = 3,5-$(CF_3)_2C_6H_3$) highlight the rich chemistry of vinylidene complexes that still awaits exploration [36 - 39].

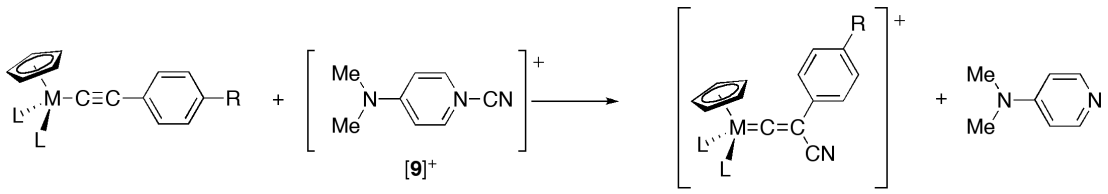

Scheme 4 A schematic representation of the synthesis of cyanovinylidene complexes from half-sandwich metal acetylide precursors and 1-cyano-4-dimethylaminopyridinium, [**9**]$^+$.

In this contribution we describe the cyanation of a range of half-sandwich acetylide complexes Ru(C≡CC_6H_4R-4)(PPh_3)$_2$Cp (R = H (**1**) [29], Me (**2**) [40, 41], OMe (**3**), CN (**4**) [42], CO_2Me (**5**)), Ru(C≡CFc)(PPh_3)$_2$Cp (**6**) [Fc = Fe(η-C_5H_4)(η-C_5H_5)] [43, 44] and the iron complexes Fe(C≡CC_6H_4R-4)(dppe)Cp (R = H (**7**) [41, 45], Me (**8**) [41] by 1-cyano-4-dimethylaminopyridinium tetrafluoroborate ([**9**]BF_4) (Scheme 4). These synthetic studies are augmented by molecular structure determinations, electrochemical measurements and representative IR spectroelectrochemical studies. In addition to the structures of the key reagent [**9**]BF_4 and several of the cyanovinylidene products, the structures of two of the acetylide precursors, Ru(C≡CC_6H_4OMe-4)(PPh_3)$_2$Cp (**3**) and Ru(C≡C$C_6H_4CO_2$Me-4)(PPh_3)$_2$Cp (**5**), were also determined, and are briefly described here for completeness. DFT based computational studies on representative cyanovinylidene complexes have also been carried out, which together with the structural, electrochemical and spectroscopic data provide insight into the electronic structure of the cyanovinylidene ligand. Preliminary results in this area from our group has been communicated previously [46].

2. Experimental section

2.1 General conditions All reactions were carried out in oven dried (110 ºC) glassware and in a dry high-purity nitrogen environment, using standard Schlenk techniques. Solvents were dried on an Innovative Technologies SPS-400 system and degassed prior to use. The compounds HC≡CC_6H_4OMe-4 [47], HC≡$CC_6H_4CO_2$Me-4 [48], $RuCl(PPh_3)_2Cp$ [49], [Ru(C≡CC_6H_5)$(PPh_3)_2Cp$] [50], [Ru(C≡CC_6H_4Me-4)$(PPh_3)_2Cp$] [40], [Ru(C≡CC_6H_4CN-4)$(PPh_3)_2Cp$] [42], and [Ru(C≡CFc)$(PPh_3)_2Cp$] [43], were prepared according the literature methods. BrCN was freshly sublimed under nitrogen in a water bath at 60ºC prior to use. All other reagents were used as received. Preparative TLC was carried out on silica gel, GF_{254}, 20 x 20 cm plates.

NMR spectra were obtained using Varian Mercury-200 (^{1}H, 199.99 MHz; ^{13}C, 49.98 MHz; ^{19}F 188.18 MHz; ^{31}P, 80.96 MHz), Bruker and Varian Mercury-400 (^{1}H, 399.97 MHz; ^{13}C, 100.57 MHz; ^{19}F, 376.36 MHz; ^{31}P, 161.10 MHz), Varian Inova-500 (^{1}H, 499.77 MHz, ^{13}C, 125.67 MHz; ^{19}F 470.25 MHz; ^{31}P, 202.31 MHz) or Varian VNMRS-700 (^{1}H, 699.73 MHz, ^{13}C, 175.95 MHz ; ^{19}F 658.41 MHz; ^{31}P, 279.89 MHz) spectrometers in $CDCl_3$, unless otherwise stated, and referenced against solvent references (^{1}H, 7.26 ppm; ^{13}C, 77.0 ppm) or external H_3PO_4 (^{31}P) and $CFCl_3$ (^{19}F). Mass spectra were obtained using a Waters Micromass LCT mass spectrometer. Infrared spectra were recorded in solution cells fitted with CaF_2 windows on a Nicolet Avatar FT-IR spectrometer.

Electrochemical measurements (Autolab PG-STAT 30) were carried out using CH_2Cl_2 solutions containing 0.1 M NBu_4BF_4 electrolyte in a standard three-electrode cell using Pt electrodes, and potentials are reported on the SCE scale using an internal

ferrocene/ferrocenium couple (Fc/Fc^+ = 0.45 V) or decamethylferrocene/decamethylferrocenium couple (Fc^*/Fc^{*+} = –0.07 V) as reference. Spectroelectrochemical studies were conducted at room temperature using a gas-tight cell fitted with CaF_2 windows, Pt gauze working electrode, Ag-wire pseudo reference and Pt counter electrodes [51].

All *ab initio* computations were carried out with the Gaussian 09 package [52]. The model geometries were optimised using the B3LYP functional [53, 54], with the 3-21G* basis set [55, 56]. Frequency calculations were computed on these optimised geometries and shown to have no imaginary frequencies. A scaling factor of 0.95 was applied to the calculated vibrational frequencies for comparison with experimental data [57, 58]. The MO diagrams and orbital contributions were generated with the aid of the GaussView 5.0 [59] and GaussSum [60] packages, respectively.

2.2 General procedure: Synthesis of Ru(C≡CC$_6$H$_4$R-4)(PPh$_3$)$_2$Cp (R = OMe, ***3****; CO$_2$Me,* ***5****)* A Schlenk flask was charged with $RuCl(PPh_3)_2Cp$ (0.20 g, 0.28 mmol), the appropriate alkyne $HC{\equiv}CC_6H_4R$-4 (ca. 0.35 mmol) and NH_4PF_6 (0.09 g, 0.5 mmol) in methanol (15 mL) and refluxed for 1 hour (R = CO_2Me) to 3 hours (R = OMe). The resulting red solution was cooled, treated with a few drops of DBU, and stirred for 10 minutes in an ice-water bath. The resulting yellow precipitate was collected by filtration, washed with methanol (3 × 5 mL) and dried in vacuo. Recrystallisation from acetone / hexane affords crystals suitable for X-ray crystallography.

*2.2.1. Ru(C≡CC$_6$H$_4$OMe-4)(PPh$_3$)$_2$Cp **3*** Yield 57%. $C_{50}H_{42}OP_2Ru$ requires: C, 73.07; H, 5.15%. Found: C, 73.64; H, 5.27%. IR (CH_2Cl_2, cm^{-1}): *v*(C≡C) 2077(s). ^{1}H NMR: δ 3.77 (s, 3H, CH_3), 4.30 (s, 5H, Cp), 6.70 (d, $^3J_{HH}$ = 8 Hz, 2H, H5/7), 7.07 (m, 14H, H4/8, *meta*-CH of PPh_3), 7.16 (m, 6H, *para*-CH of PPh_3), 7.48 (m, 12H, *ortho*-CH of PPh_3). ^{13}C{^{1}H} NMR: δ 55.2 (s, CH_3), 85.0 (s, Cp), 111.6 (t, $^2J_{CP}$ = 25 Hz, C_α), 113.2 (s, C_β), 113.2, 123.5, 131.5, 155.8 (4 × s, C3 - C8), 127.1 (dd, $^3J_{CP}$/$^5J_{CP}$ = 4 Hz, *meta*-C of PPh_3), 128.3 (s, C_p), 133.8 (dd, $^2J_{CP}$/$^4J_{CP}$ = 5 Hz, *ortho*-C of PPh_3), 138.9 (m, *ipso*-C of PPh_3), ^{31}P{^{1}H} NMR: δ 51.4 (s). ES(+)-MS (*m/z*): 823 $[M + H]^+$, 691 $[Ru(PPh_3)_2Cp]^+$.

*2.2.2. Ru(C≡CC$_6$H$_4$CO$_2$Me-4)(PPh$_3$)$_2$Cp **5*** Yield 58%. $C_{51}H_{42}O_2P_2Ru$ requires: C, 72.07; H, 4.98 %. Found: C, 72.62; H, 4.95 % IR (CH_2Cl_2, cm^{-1}): *v*(C≡C) 2067(s); v(C=O) 1707(s); v(C-O) 1595(s). ^{1}H NMR: δ 3.88 (s, 3H, CH_3), 4.34 (s, 5H, Cp), 7.07 (m, 14H, H4/8 and *meta*-CH of PPh_3), 7.18 (m, 6H, *para*-CH of PPh_3), 7.44 (m, 12H, *ortho*-CH of PPh_3), 7.80 (d, $^3J_{HH}$ = 8 Hz, 2H, H5/7). ^{13}C{^{1}H} NMR: δ 51.7 (s, CH_3), 85.3 (s, Cp), 115.7 (s, C2), 123.8, 129.3, 130.1, 135.3 (4 × s, C3 - C8), 127.3 (dd, $^3J_{CP}$/$^5J_{CP}$ = 5 Hz, *meta*-C of PPh_3), 128.2 (s, C_p), 133.7 (dd, $^2J_{CP}$/$^4J_{CP}$ = 5 Hz, *ortho*-C of PPh_3), 138.6 (m, *ipso*-C of PPh_3), 167.5 (s, C=O). C1 not observed. ^{31}P{^{1}H} NMR: δ 51.3 (s). ES(+)-MS (*m/z*): 851 $[M + H]^+$, 691 $[Ru(PPh_3)_2Cp]^+$.

*2.3 General procedure: Synthesis of Fe(C≡CC$_6$H$_4$-4)(dppe)Cp (R = H, **7**; Me, **8**)* A solution of FeCl(dppe)Cp (200 mg, 0.36 mmol) in methanol (15 ml) was treated with the appropriate alkyne HC≡CC$_6$H$_4$R-4 (several drops, excess) and the dark reaction solution heated at gentle reflux for ca. 1 hr. During this time the solution colour changed to a deep, translucent red characteristic of the vinylidene complex

[Fe{C=C(H)C_6H_4R-4}(dppe)Cp]Cl. The solution was allowed to cool to room temperature before being treated with several drops of DBU, causing the solution colour to change to bright orange. Cooling the solution in an ice/water bath caused the precipitation of Fe(C≡CC_6H_4R-4)(dppe)Cp as a bright orange precipitate (R = H, 75%; R = Me, 80%), identified by comparison with the literature data [41].

*2.4 Synthesis of 1-cyano-4-dimethylaminopyridinium tetrafluoroborate, [**9**]BF_4* A Schlenk flask was charged with BrCN (1.09 g, 10.3 mmol) in NCMe (45 ml) and 4-dimethylaminopyridine (1.00 g, 8.22 mmol) was then added. The reaction mixture was allowed to stir for 5 min., before the addition of $NaBF_4$ (1.08 g, 9.79 mmol). After stirring for a further 2.5 hours, the reaction mixture was filtered through a Celite plug and concentrated to dryness to give a white powder. The powder was dissolved in NCMe (15 ml), stirred for 3 min. and then filtered again through a Celite plug. After concentrating to dryness, the extraction process was repeated for a final time. Concentration to dryness and recrystallisation from NCMe/EtOAc afforded needle-like, white crystals (1.23 g, 64%). Single crystals suitable for X-ray diffraction were obtained by slow diffusion of ethyl acetate into a concentrated NCMe solution of the salt. $C_8H_{10}N_3BF_4$ requires: C, 40.89; H, 4.29; N, 17.88 %. Found: C, 40.89; H, 4.26; N, 17.88 %. IR (nujol, cm^{-1}): *ν*(C≡N) 2264(m); *ν*(CC) 1655(s). ^{1}H NMR (CD_3CN): δ 3.34 (s, 6H, CH_3); 7.02, 8.09 (2 × d, *J* = 8 Hz, 2 × 2H, C_5H_4N). $^{13}C\{^1H\}$ NMR (CD_3CN): δ 42.3 (s, CH_3), 107.7 (s, CN), 108.5, 141.5, 158.1 (3 × s, C_5H_4N). ^{19}F NMR (CD_3CN): δ –152.3 (s, BF_4^-). ES(+)-MS (*m/z*): 148 $[Me_2NC_5H_4NCN]^+$, 123 $[Me_2NC_5H_4NH]^+$.

2.5 General procedure: Synthesis of cyanovinylidene complexes A Schlenk flask was charged with the appropriate metal acetylide complex (ca. 0.1 mmol) in CH_2Cl_2 (10 ml). A separate Schlenk flask was charged with one-equivalent of [**9**]BF_4 in NCMe (5 ml). The [**9**]BF_4 solution was transferred by syringe to the solution of the acetylide and the reaction mixture stirred for 2 hours. The resulting cherry red solution was concentrated to dryness, and the residue purified by preparative TLC (acetone/hexane, 6/4). The major orange/red band was collected and isolated as a red solid by precipitation or crystallisation.

2.5.1. [Ru{C=C(CN)Ph}(PPh$_3$)Cp]BF$_4$ [**11**]BF_4 crystallised from acetone / hexane. Yield 80%. $C_{50}H_{40}NP_2RuBF_4$ requires: C, 66.38; H, 4.46; N, 1.55. Found: C, 66.48; H, 4.00; N, 1.36. IR (CH_2Cl_2, cm^{-1}): *ν*(C≡N) 2202(s); *ν*(C=C) 1582(s). ^{1}H NMR: δ 5.41 (s, 5H, Cp); 6.95 (d, 2H, $^3J_{HH}$ ~ 8 Hz, H4/8); 7.01 (m, 12H, *ortho*-CH of PPh_3); 7.22 (*pseudo*-t, 2H, $^3J_{HH}$ ~ 8 Hz, H5/7); 7.30 (m, 14H, H6, *meta*-CH of PPh_3); 7.43 (m, 6H, *para*-CH of PPh_3). ^{13}C NMR: δ 96.6 (s, Cp); 109.6, 109.7 (2 × s, CN, C2); 123.6, 127.4, 128.7, 129.3 (4 × s, C3 - C8); 128.9 (dd, $^3J_{CP,}$ $^5J_{CP}$ ~ 5 Hz, *meta*-C of PPh_3); 131.5 (s, C_p); 132.2 (m, *ipso*-C of PPh_3); 133.6 (dd, $^2J_{CP,}$ $^4J_{CP}$ ~ 5 Hz, *ortho*-C of PPh_3); 348.5 (t, $^2J_{CP}$ = 16 Hz, C1). ^{31}P{^{1}H} NMR: δ 38.8 (s). ^{19}F{^{1}H} NMR: δ –153.0 (s, BF_4^-). ^{11}B{^{1}H} NMR: δ –0.7 (s, BF_4^-). ES(+)-MS (*m/z*): 857, [Ru{C=C(CN)Ph}$(PPh_3)_2$Cp+K]$^+$; 818 [Ru{C=C(CN)Ph}$(PPh_3)_2$Cp]$^+$.

2.5.2. [Ru{C=C(CN)C$_6$H$_4$Me-4}(PPh$_3$)$_2$Cp]BF$_4$ [**12**]BF_4 precipitated from CH_2Cl_2 / Et_2O as a red powder. Yield 90%. $C_{51}H_{42}NP_2RuBF_4$ requires: C, 66.67; H, 4.61, N, 1.52 %. Found: C, 67.01; H, 4.89; N, 1.46 %. IR (acetone, cm^{-1}): ν(C≡N) 2200(s); ν(C=C) 1580(s). ^{1}H NMR: δ 2.35 (s, 3H, CH_3); 5.38 (s, 5H, Cp); 6.81, 7.09 (2 × d, 2

× 2H, $^{3}J_{HH}$ ~ 8 Hz, C_6H_4); 7.02 (m, 12H, *ortho*-CH of PPh_3); 7.31 (m, 12H, *meta*-CH of PPh_3); 7.44 (m, 6H, *para*-CH of PPh_3). ^{13}C NMR: δ 21.1 (s, CH_3); 96.6 (s, Cp), 109.5, 109.8 (2 × s, CN, C2); 120.1, 127.5, 130.1, 138.9 (4 × s, C3-C8); 128.9 (dd, $^{3}J_{CP,}$ $^{5}J_{CP}$ ~ 5 Hz, *meta*-C of PPh_3); 131.5 (s, *para*-C of PPh_3); 132.2 (m, *ipso*-C of PPh_3); 133.5 (dd, $^{2}J_{CP,}$ $^{4}J_{CP}$ ~ 5 Hz, *ortho*-C of PPh_3); 349.3 (t, $^{2}J_{CP}$ = 16 Hz, C1). ^{31}P{H} ($CDCl_3$): δ 38.9 (s). ES(+)MS (*m/z*) 833 [Ru{C=C(CN)C_6H_4Me-4}$(PPh_3)_2$Cp]$^{+}$.

2.5.3. [Ru{C=C(CN)C_6H_4OMe-4}$(PPh_3)_2$Cp]BF_4 [**13**]BF_4 crystallised from acetone/Et_2O. Yield 50%. $C_{51}H_{42}NOP_2RuBF_4$.$(CH_3)_2CO$ requires: C, 65.33; H, 4.87, N, 1.41 %. Found: C, 64.49; H, 4.41; N, 1.47 %. IR (CH_2Cl_2, cm^{-1}): *ν*(C≡N) 2201(m); *ν*(C=C) 1595(m). ^{1}H NMR: δ 3.75 (s, 3H, CH_3); 5.37 (s, 5H, Cp), 6.85 (br, 4H, C_6H_4), 7.00 (m, 12H, *ortho*-CH of PPh_3); 7.30 (m, 12H, *meta*-CH of PPh_3); 7.41 (m, 6H, *para*-CH of PPh_3). ^{13}C NMR: δ 55.5 (CH_3); 96.5 (s, Cp); 108.7, 109.7 (2 × s, CN, C2); 114.2, 115.0, 129.4, 160.2 (C3 - C8), 128.9 (dd, $^{3}J_{CP,}$ $^{5}J_{CP}$ ~ 5 Hz, *meta*-C of PPh_3), 131.5 (s, *para*-C of PPh_3), 132.4 (m, *ipso*-C of PPh_3), 133.6 (dd, $^{2}J_{CP,}$ $^{4}J_{CP}$ ~ 5 Hz, *ortho*-C of PPh_3), 349.2 (t, $^{2}J_{CP}$ = 15 Hz, C1). ^{31}P{^{1}H} NMR ($CDCl_3$): δ 39.1 (s). ES(+)-MS (*m/z*): 848 [Ru{C=C(CN)C_6H_4OMe-4}$(PPh_3)_2$Cp]$^{+}$.

2.5.4. [Ru{C=C(CN)C_6H_4CN-4}$(PPh_3)_2$Cp]BF_4 [**14**]BF_4 crystallised from acetone/hexane. Yield 67%. $C_{51}H_{39}N_2P_2RuBF_4$.2.5$(CH_3)_2CO$ requires: C, 64.47; H, 4.84, N, 2.64 %. Found: C, 64.94; H, 4.87; N, 2.67 %. IR (CH_2Cl_2, cm^{-1}): *ν*(C≡N) 2230(m), 2202(m); *ν*(C=C) 1603(m), 1571(s). ^{1}H NMR: δ 5.52 (s, 5H, Cp); 7.02 (m, 12H, *ortho*-CH of PPh_3); 7.08, 7.50 (2 × d, 2 × 2H, $^{3}J_{HH}$ ~ 8 Hz, C_6H_4); 7.32 (m, 12H, *meta*-CH of PPh_3); 7.46 (m, 6H, *para*-CH of PPh_3). ^{13}C NMR: δ 97.2 (s, Cp); 109.1,

109.5 (2 × s, CN, C2); 111.3, 126.7, 129.8, 132.7 (4 × s, C3 - C8); 118.3 (C_6H_4CN); 129.0 (dd, $^3J_{CP,}$ $^5J_{CP}$ ~ 5 Hz, *meta*-C of PPh_3); 131.6 (s, C_p); 131.8 (m, *ipso*-C of PPh_3); 133.5 (dd, $^2J_{CP,}$ $^4J_{CP}$ ~ 5 Hz, *ortho*-C of PPh_3), 346.5 (t, $^2J_{CP}$ = 14 Hz, C1). $^{31}P\{^1H\}$ NMR: δ 37.7 (s). ES(+)-MS (*m/z*): 843 $[Ru\{C=C(CN)C_6H_4CN\text{-}4\}(PPh_3)_2Cp]^+$.

2.5.5. [Ru{C=C(CN)C$_6$H$_4$CO$_2$Me-4}(PPh$_3$)$_2$Cp]BF$_4$ [**15**]BF_4 crystallised from acetone / hexane. Yield 45 %. $C_{52}H_{42}NO_2P_2RuBF_4$ requires: C, 66.67; H, 4.61, N, 1.52 %. Found: C, 64.00; H, 4.40; N, 1.46 %. IR (CH_2Cl_2, cm^{-1}): *ν*(C≡N) 2203(m); *ν*(C=O) 1721; *ν*(C=C) 1607(m), 1578(s). ^1H NMR: δ 3.92 (s, 3H, CH_3); 5.49 (s, 5H, Cp); 7.01 (m, 14H, H4/8 and *ortho*-CH of PPh_3), 7.32 (m, 12H, *meta*-CH of PPh_3), 7.45 (m, 6H, *para*-CH of PPh_3), 7.89 (d, 2H, $^3J_{HH}$ ~ 8 Hz, H5/7). ^{13}C NMR: δ 52.3 (CH_3); 96.9 (s, Cp); 109.4, 109.8 (2 × s, CN, C2); 126.2 129.4, 129.7, 130.3 (4 × s, C3 - C8); 128.9 (dd, $^3J_{CP,}$ $^5J_{CP}$ ~ 5 Hz, *meta*-C of PPh_3); 131.7 (s, *para*-C of PPh_3); 132.2 (m, *ipso*-C of PPh_3); 133.6 (dd, $^2J_{CP,}$ $^4J_{CP}$ ~ 5 Hz, *ortho*-C of PPh_3); 166.2 (s, C=O); 347.9 (t, $^2J_{CP}$ = 15 Hz, C1). $^{31}P\{^1H\}$ NMR: δ 38.1 (s). ES(+)-MS (*m/z*): 876 $[Ru\{C=C(CN)C_6H_4CO_2Me\text{-}4\}(PPh_3)_2Cp]^+$.

2.5.6. [Ru{C=C(CN)Fc}(PPh$_3$)$_2$Cp]BF$_4$ [**16**]BF_4 crystallised from acetone / hexane. Yield 75%. $C_{54}H_{44}NP_2RuFeBF_4$ requires: C, 64.05; H, 4.39, N, 1.38 %. Found: C, 63.67; H, 4.38; N, 1.34 %. IR (CH_2Cl_2, cm^{-1}): *ν*(C≡N) 2220, 2205(w), *ν*(C=C) 1593 (s). ^1H NMR: δ 3.68, 4.10 (4H, C_5H_4); 4.15 (s, 5H, CpFe); 4.71 (s, 5H, CpRu); 6.82 (m, 12H, *ortho*-CH of PPh_3); 7.30 (m, 12H, *meta*-CH of PPh_3); 7.41 (m, 6H, *para*-CH of PPh_3). ^{13}C NMR: δ 67.5, 69.3, 72.1 (3 × s, C_5H_4); 70.1 (FeCp); 95.9 (RuCp); 106.3, 109.5 (2 × s, CN, C2); 128.7 (dd, $^3J_{CP,}$ $^5J_{CP}$ ~ 5 Hz, *meta*-C of PPh_3); 131.5 (s, *para*-C

of PPh_3); 132.3 (m, *ipso*-C of PPh_3); 133.1 (dd, $^2J_{CP,}$ $^4J_{CP}$ ~ 5 Hz, *ortho*-C of PPh_3); 347.1 (t, $^2J_{CP}$ = 15 Hz, C1). $^{31}P\{^1H\}$ NMR ($CDCl_3$): δ 39.8 (s). ES(+)-MS (*m/z*): 926 $[Ru\{C=C(CN)Fc\}(PPh_3)_2Cp]^+$.

2.5.7. [Fe{C=C(CN)C$_6$H$_5$}(dppe)Cp]BF$_4$ [**17**]BF_4 crystallised from methanol. Yield 60%. $C_{40}H_{34}NP_2FeBF_4$ requires: C, 65.52; H, 4.67; N, 1.91. Found: C, 65.01; H, 4.58; N, 1.89 %. IR (CH_2Cl_2, cm^{-1}): ν(C≡N) 2202(s); ν(C=C) 1584(s). ^1H NMR ($(CD_3)_2CO$) δ 3.30 (m, 2H, dppe); 3.43 (m, 2H, dppe); 5.82 (s, 5H, Cp); 6.76, 7.04, 7.05 (3 × m, C_6H_5); 7.34 (m, 8H, dppe), 7.45 (m, 6H, dppe), 7.62 (m, 6H, dppe). ^{13}C NMR ($(CD_3)_2CO$): δ 27.3 (m, CH_2); 90.8 (s, Cp); 108.3 (t, $^4J_{CP}$ = 4 Hz, C2), 118.1 (s, CN); 123.5 (t, $^5J_{CP}$ = 2 Hz, C3); 126.6, 128.0, 128.8 (C4 - C8); 128.0, 128.3 (2 × dd, $^3J_{CP}$, $^5J_{CP}$ ~ 5 Hz, *meta*-C, C' of dppe); 130.5, 130.6 (2 ×s, *para*-C, C' of dppe); 130.6, 131.5 (2 × dd, $^2J_{CP,}$ $^4J_{CP}$ ~ 5 Hz, *ortho*-C, C' of dppe); 132.6, 134.0 (2 × m, *ipso*-C, C' of dppe), 355.2 (t, J_{CP} = 34 Hz, C1). ^{31}P NMR ($(CD_3)_2CO$) δ 92.1. ES(+)-MS (*m/z*): 646, $[Fe\{C=C(CN)C_6H_5\}(dppe)Cp]^+$.

2.5.8 [Fe{C=C(CN)C$_6$H$_4$Me-4}(dppe)Cp]BF$_4$ [**18**]BF_4 crystallised from methanol. Yield 40%. $C_{41}H_{36}NP_2FeBF_4$ requires: C, 65.89; H, 4.86; N, 1.87. Found: C, 64.96; H, 4.66; N, 2.10 %. IR (CH_2Cl_2, cm^{-1}): ν(C≡N) 2202(s); ν(C=C) 1584(s). ^1H NMR: δ 2.21 (s, 3H, CH_3); 3.03 (m, 2H, dppe); 3.10 (m, 2H, dppe); 5.36 (s, 5H, Cp); 6.49, 6.77 (2 × d, $^3J_{HH}$ = 8 Hz, C_6H_4); 7.07, 7.20, 7.29, 7.38 (4 × m, 20H, dppe). ^{13}C NMR: δ 21.0 (s, CH_3); 28.3 (m, CH_2); 91.4 (s, Cp); 109.7 (t, $^4J_{CP}$ = 4 Hz, C2); 119.1 (CN); 120.1 (t, $^5J_{CP}$ = 2 Hz, C3), 125.4, 129.9, 137.9 (C4-C8); 129.3, 129.5 (2 × dd, $^3J_{CP}$, $^5J_{CP}$ ~ 5 Hz, *meta*-C, C' of dppe), 131.7, 131.8 (2 ×s, *para*-C, C' of dppe), 131.3, 132.1 (2 × dd, $^2J_{CP,}$ $^4J_{CP}$ ~ 5 Hz, *ortho*-C, C' of dppe), 132.5, 134.1 (2 × m, *ipso*-C, C'

of dppe), 357.5 (t, J_{CP} = 33 Hz, C1). ^{31}P NMR: δ 91.0. ES(+)-MS (*m/z*): 660, [Fe{C=C(CN)C_6H_4Me-4}(dppe)Cp]$^+$.

2.6. Synthesis of [Ru{C=C(CN)C_6H_4R-4}(PPh_3)$_2$Cp]PF_6 (R = H, [**11**]PF_6; *Me,* [**12**]PF_6*)* To a solution of BrCN (30 mg, 0.31 mmol) in CH_2Cl_2 (2 ml), was added 4-dimethylaminopyridine (80 mg, 0.31 mmol) and the solution was stirred for 5 min to give a solution containing [CAP]Br. To this, a solution of Ru(C≡CC_6H_4R-4)(PPh_3)$_2$Cp (0.12 mmol) in CH_2Cl_2 (4 ml) was added via cannula and the solution stirred for 5 min. Then NH_4PF_6 (300 mg, 1.84 mmol) was added, the solution was filtered and the solvent was removed *in vacuo*. Purification the red residue by preparative TLC (acetone/hexane 6:4) gave a major red band which was collected and crystallised (R = H, acetone / hexane, 50%; R = Me, acetone / Et_2O, 46%). Spectroscopic data were consistent with those of the BF_4^- salt.

2.7 Synthesis of FeCl(dppe)Cp [61]. A solution of dppe (5.06 g, 12.7 mmol) in $CHCl_3$ (30 ml) was transferred into a solution of $FeCl_2.4H_2O$ (2.51 g, 12.6 mmol) in acetone (120 ml). The resulting brown solution was heated at reflux for ca. 20 h. After this time the white precipitate that had formed was collected by filtration, washed with three portions of Et_2O and dried to give $FeCl_2$(dppe) (5.43 g, 82%). This paramagnetic, high-spin tetrahedral complex was identified by atmospheric solids analysis probe mass spectrometry (ASAP-MS, *m/z* 524.0, [M]$^+$) and used directly in the next step. A Schlenk flask was charged with $FeCl_2$(dppe) (2.78 g, 5.30 mmol), TlCp (1.33 g, 4.95 mmol) (CARE: Thallium salts are highly toxic) and benzene (50 ml). The resulting suspension was allowed to stir overnight to give a characteristically deep purple coloured solution, which was filtered through Celite to remove

precipitated TlCl (CARE!) and unreacted $FeCl_2$(dppe). The solvent was removed and the dark coloured residue dissolved in the minimum volume of CH_2Cl_2. Addition of an equal volume of Et_2O resulted in the almost immediate on set of crystallisation of FeCl(dppe)Cp. When crystallisation was complete (several hours) the resulting crystalline mass was collected by filtration, washed with Et_2O, hexane and finally a second portion of Et_2O and dried to give the desired product (2.34 g, 85%).

2.8 X-ray structure determinations

Single crystal X-ray data were collected at 120K on the Rigaku R-Axis Spider IP ([**18**]BF_4), Bruker SMART 1K ([**11**]PF_6) and Bruker SMART 6000 (all other reported compounds) diffractometers, equipped with the Cryostream (Oxford Cryosystems) nitrogen cooling devices and using graphite monochromated MoK_α radiation (Mo-Kα, λ = 0.71073Å). The structures were solved by direct method and refined by full-matrix least squares on F^2 for all data using SHELXTL [62] and OLEX2 [63] software. All non-disordered non-hydrogen atoms were refined with anisotropic displacement parameters, H-atoms were placed in the calculated positions and refined in riding mode in all structures except [**9**]BF_4 and [**18**]BF_4, where they were refined isotropically.

*Crystal data for **3***: $C_{50}H_{42}OP_2Ru$, M = 821.85, triclinic, space group P -1, a = 15.0237(3), b = 17.1759(3), c = 17.2624(3) Å, α = 116.31(1), β = 96.20(1), γ = 98.22(1)° U = 3877.8(1) $Å^3$, F(000) = 1696, Z = 4, D_c = 1.408 mg m^{-3}, μ = 0.525 mm^{-1}. 47012 reflections were collected yielding 18680 unique data (R_{merg} = 0.0397). Final $wR_2(F^2)$ = 0.0843 for all data (973 refined parameters), conventional R_1 (F) = 0.0336 for 14573 reflections with $I \geq 2\sigma$, GOF = 1.030.

Crystal data for ***5***: $C_{51}H_{42}O_2P_2Ru$, M = 849.86, monoclinic, space group P 2_1, a = 8.9199(3), b = 14.7736(4), c = 15.1537(4)Å, β = 90.13(1)°, U = 1996.9(1)Å^3, F(000) = 876, Z = 2, D_c = 1.413 mg m^{-3}, μ = 0.515 mm^{-1}. 19700 reflections were collected yielding 9572 unique data (R_{merg} = 0.0372). Final $wR_2(F^2)$ = 0.1103 for all data (505 refined parameters), conventional $R_1(F)$ = 0.0451 for 8437 reflections with I ≥ 2σ, GOF = 1.077.

Crystal data for [**9**]BF_4: $C_8H_{10}N_3 \times BF_4$, M = 235.00, orthorhombic, space group P bca, a = 9.0261(4), b = 11.0956(5), c = 20.2847(10) Å, U = 2031.51(16) Å^3, F(000) = 960, Z = 8, D_c = 1.537 mg m^{-3}, μ = 0.146 mm^{-1}. 20483 reflections were collected yielding 2218 unique data (R_{merg} = 0.0214). Final $wR_2(F^2)$ = 0.1597 for all data (185 refined parameters), conventional $R_1(F)$ = 0.0571 for 2002 reflections with I ≥ 2σ, GOF = 1.096.

Crystal data for [**11**]PF_6: $C_{50}H_{40}NP_2Ru \times PF_6 \times (CH_3)_2CO$, M = 1020.89, orthorhombic, space group P bca, a = 18.1453(5), b = 14.1423(4), c = 36.0979(9) Å, U = 9263.3(4) Å^3, F(000) = 4176, Z = 8, D_c = 1.464 mg m^{-3}, μ = 0.507 mm^{-1}. 81086 reflections were collected yielding 12115 unique data (R_{merg} = 0.0825). Final $wR_2(F^2)$ = 0.0947 for all data (586 refined parameters), conventional $R_1(F)$ = 0.0403 for 8359 reflections with I ≥ 2σ, GOF = 1.027.

Crystal data for [**12**]PF_6: $C_{51}H_{42}NP_2Ru \times PF_6 \times (CH_3)_2CO$, M = 1034.91, monoclinic, space group P $2_1/n$, a = 10.0492(2), b = 35.6830(7), c = 12.9509(3) Å, β = 99.04(1)°, U = 4586.3(2) Å^3, F(000) = 2120, Z = 4, D_c = 1.499 mg m^{-3}, μ = 0.513 mm^{-1}. 65840 reflections were collected yielding 14617 unique data (R_{merg} = 0.0572). Final $wR_2(F^2)$

= 0.0928 for all data (595 refined parameters), conventional $R_1(F)$ = 0.0337 for 11738 reflections with $I \geq 2\sigma$, GOF = 1.068.

Crystal data for [**14**]BF_4: $C_{51}H_{39}N_2P_2Ru \times BF_4 \times 2.5(CH_3)_2CO$, M = 1034.91, monoclinic, space group C 2/c, a = 37.8522(8), b = 14.9728(3), c = 36.7338(8) Å, β = 99.48(1)°, U = 20534.6(7) $Å^3$, F(000) = 8480, Z = 16, D_c = 1.334 mg m^{-3}, μ = 0.424 mm^{-1}. 116691 reflections were collected yielding 31305 unique data (R_{merg} = 0.0584). Final $wR_2(F^2)$ = 0.2239 for all data (1035 refined parameters), conventional $R_1(F)$ = 0.0666 for 20178 reflections with $I \geq 2\sigma$, GOF = 1.050.

Crystal data for [**18**]BF_4: $C_{41}H_{36}NP_2Fe \times BF_4$, M = 747.31, orthorhombic, space group P bca, a = 15.7333(16), b = 16.6689(17), c = 26.302(3) Å, U = 6897.8(12) $Å^3$, F(000) = 3088, Z = 8, D_c = 1.439 mg m^{-3}, μ = 0.584 mm^{-1}. 57139 reflections were collected yielding 9160 unique data (R_{merg} = 0.0777). Final $wR_2(F^2)$ = 0.1105 for all data (595 refined parameters), conventional $R_1(F)$ = 0.0488 for 7354 reflections with $I \geq 2\sigma$, GOF = 1.090.

3. Results and Discussion

3.1 Synthesis and structures of half-sandwich acetylide precursors

Treatment of $RuCl(PPh_3)_2Cp$ with the appropriate alkyne $HC{\equiv}CC_6H_4R$-4 and NH_4PF_6 in methanol gave the vinylidene complexes $[Ru\{C{=}C(H)C_6H_4R\text{-}4\}(PPh_3)_2Cp]PF_6$ which were deprotonated in situ to give the desired acetylide complexes $Ru(C{\equiv}CC_6H_4R\text{-}4)(PPh_3)_2Cp$ (**1** - **5**) in the well-established manner [29]. The ferrocenyl substituted derivative $Ru(C{\equiv}CFc)(PPh_3)_2Cp$ (**6**) [43, 44] and the iron

complexes **7** and **8** were prepared similarly from FeCl(dppe)Cp and the appropriate alkyne, and characterised by comparison with literature data [41, 45]. In the case of the iron complexes, the Fe-Cl bond was sufficiently ionised in methanol to promote smooth formation of the intermediate vinylidene without the need for a supporting salt to act as halide scavenging agent [64, 65] or the use of the acetonitrile complex $[Fe(NCMe)(dppe)Cp]PF_6$ [45]. This simple procedure also avoids the use of ligand exchange steps either in the preparation of FeI(dppe)Cp as a precursor [66 - 68], or in the preparation of phosphine-ligand acetylide complexes from $Fe(C{\equiv}CR)(CO)_2Cp$ [69 - 71]. The key precursor FeCl(dppe)Cp is in turn very easily accessed from reaction of hydrated ferrous chloride with dppe to give $FeCl_2$(dppe), followed by treatment with TlCp (Scheme 5) [61]. It was most convenient to carry out the last step with a small excess of $FeCl_2$(dppe), to prevent the formation of ferrocene and liberation of dppe, the latter proving to be rather difficult to separate from the half-sandwich product. The excess insoluble $FeCl_2$(dppe) is simply removed from the reaction mixture by filtration with the precipitated TlCp, and the crude reaction mixture crystallised from CH_2Cl_2 / Et_2O to afford well-shaped blocks of FeCl(dppe)Cp, thereby avoiding chromatographic purification [61].

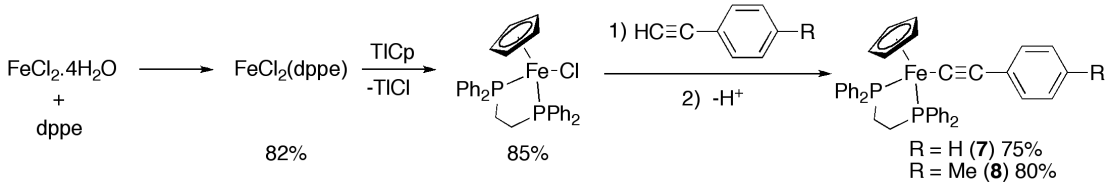

Scheme 5 The preparation of FeCl(dppe)Cp and related acetylide complexes.

3.2 Molecular structures of acetylide complexes

The molecular structures of Ru(C≡CC_6H_4OMe-4)(PPh_3)$_2$Cp (**3**) (Figure 1) and Ru(C≡C$C_6H_4CO_2$Me-4)(PPh_3)$_2$Cp (**5**) (Figure 2) were determined and offer the same general trends as observed in other acetylide complexes based on the Ru(PPh_3)$_2$Cp moiety (Table 1) [28, 42, 72 - 80], and together permit the limited influence of the electron donating or withdrawing substitutents on the structure to be demonstrated. This is of some interest as the structures of ruthenium acetylide complexes Ru(C≡CC_6H_4R)(L)$_2$Cp' featuring electron-donating R groups are surprisingly rare in comparison with the large number of examples of systems featuring more electron-withdrawing substituents [81]. In each case (**3**, **5**) the metal centre is in a pseudo-octahedral geometry, with the P(1)-Ru-P(2) bond angle ca. 100 ° and the P(1,2)-Ru-C(1) angles ca. 90°. The Ru-C(1)≡C(2)-C(3) fragments in **3** and **5** are essentially linear, and the Ru-C(1), C(1)-C(2), C(2)-C(3) bond lengths are indistinguishable between the two complexes. The relatively precisely determined Ru-P(1,2) bond lengths provide the most informative trends, and whilst they also fall in a small range, the Ru-P bonds in **3** are at the shorter end of the range spanned by the structures established to date, reflecting the electron-donating character of the OMe substituent and the subsequently increased metal-phosphine back-bonding contribution (Table 1).

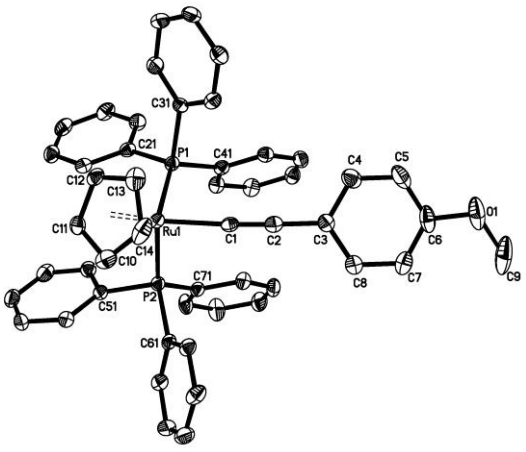

Figure 1. Molecular structure of **3** showing the atom labelling scheme.

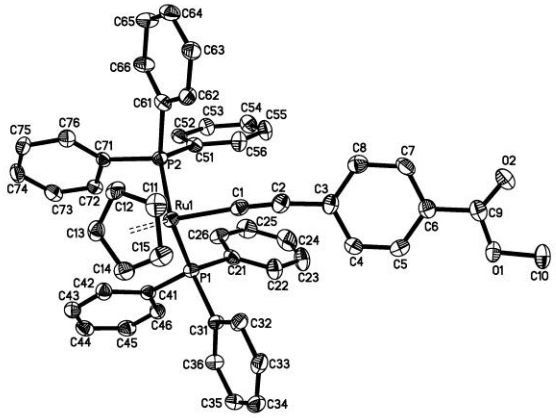

Figure 2. Molecular structure of **5** showing the atom labelling scheme.

*3.3 Selection, synthesis and structure of 1-cyano-4-dimethylaminopyridinium tetrafluoroborate ([**9**]BF_4)* It has been established earlier that cyanogen bromide, BrCN, is a useful reagent for the formation of mono and dibromovinylidenes, but not cyanated products, from metal acetylides [34], and therefore attention was turned to alternative cyanating reagents. Tosyl cyanide (*p*-tolylsulfonyl cyanide, TsCN) has been used as a cyanating reagent in reactions with organometallic compounds [82], including phenylmagnesium bromide [83] and benzylzinc halides [84], and acts as a heterodienophile in Diels-Alder reactions [85, 86]. However, reactions of **1** with TsCN in the presence of $NaPF_6$ were largely unsuccessful, with the desired monocyanovinylidene complex [Ru{C=C(Ph)CN}$(PPh_3)_2$Cp]PF_6 being obtained in only ca. 3% isolated yield.

Phenyl cyanate (cyanic acid phenyl ether, PhOCN) [87] has been used as a source of the cyano moiety in the preparation of organic [88] and organometallic [89 - 91] cyanoacetylene derivatives from acetylide anions. The reaction of **1** with PhOCN was explored under a variety of conditions. Best results were obtained from room temperature reactions of **1** with 2.5 molar equivalents of PhOCN, conducted in CH_2Cl_2. After anion methathesis, purification of the reaction mixture by preparative TLC and crystallisation of the major band, $[Ru\{C{=}C(Ph)CN\}(PPh_3)_2Cp]PF_6$ was isolated in 23% yield.

By far the most successful, widely applicable, and straightforward preparation of cyanovinylidenes was found to involve 1-cyano-4-dimethylaminopyridinium tetrafluoroborate ([**9**]BF_4) as the cyanating agent. Salts of $[\mathbf{9}]^+$ have been used in many contexts as cyanating reagents, including in the cyanation of *N*-substituted imidazoles [92], and in the cyanation of cysteine residues in proteins to inhibit the activity of cysteine active enzymes [93], and aid in peptide sequencing [94]. Solutions of the hygroscopic bromide salt [**9**]Br are readily prepared from 4-dimethylaminopyridine and cyanogen bromide [46], whilst the air-stable, crystalline BF_4^- salt, which is also available commercially, has been obtained by anion metathesis of [**9**]Br with $AgBF_4$ [93]. We found it to be expeditious to employ a small excess of cyanogen bromide in the preparation of $[\mathbf{9}]^+$ salts to ensure complete reaction of the dimethylaminopyridine which can be troublesome to remove from the products by crystallisation. In contrast, the excess volatile cyanogen bromide is simply removed during drying of the crude product in vacuo. As an alternative to anion metathesis with expensive silver salts, treatment of NCMe solutions of [**9**]Br

obtained from BrCN and dimethylaminopyridine with $NaBF_4$, followed by filtration (to remove NaBr), and recrystallisation (NCMe / EtOAc) can also be used to give crystalline [**9**]BF_4 in good (64%) yield.

*3.4 Molecular structure of 1-cyano-4-dimethylaminopyridinium tetrafluoroborate, [**9**]BF_4.*

A plot of the 1-cyano-4-dimethylaminopyridinium cation $[\mathbf{9}]^+$ is shown in Figure 3. The contraction of the N(1)-C(1) and N(3)-C(4) bonds and distortions of the pyridinium ring from an idealised aromatic towards quinoidal geometry are similar to those found in 4-dimethylaminopyridine, **10** (Figure 4) [95] and related pyridinium salts [96 - 101], with due allowance for the different temperatures used in the data collection. The cation adopts a near planar conformation, with the dimethylamino group lying just out of the aromatic plane [dihedral angles C(5)-C(4)-N(3)-C(8), 6.5(2)°; C(3)-C(4)-N(3)-C(7) 6.5(2)°]. The N(1)-C(1), C(1)-N(2), and N(3)-C(4) distances clearly distinguish the formal single, triple and single bond character of these bonds, respectively, albeit with single bonds contracted as a result of conjugation.

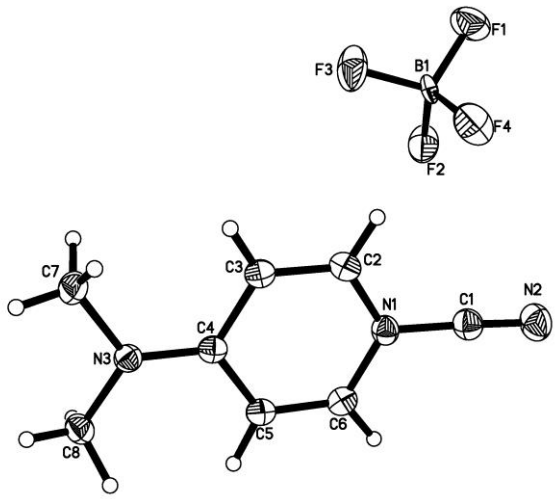

Figure 3. A plot of the ion pair in 1-cyano-4-dimethylaminopyridinium tetrafluoroborate ([**9**]BF_4). Selected bond lengths (Å) and angles (°): N(1)-C(1) 1.364(3); N(1)-C(2, 6) 1.377(3), 1.382(3); C(2)-C(3) 1.348(3); C(3)-C(4) 1.439(3); C(4)-C(5) 1.432(3); C(5)-C(6) 1.342(3); C(1)-N(2) 1.142(3); C(4)-N(3) 1.321(3); N(1)-C(1)-N(2) 177.6(3); C(4)-N(3)-C(7, 8) 121.8(2), 122.4(2); C(7)-N(3)-C(8) 115.1(2).

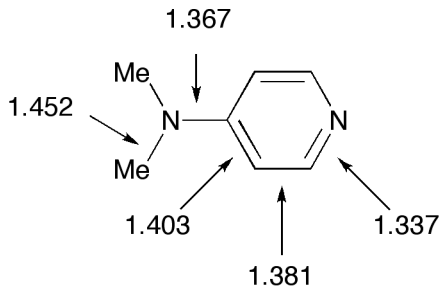

Figure 4. A sketch of 4-dimethylaminopyridine, **10**, showing selected, crystallographically determined bond lengths (Å) [95].

3.5 Synthesis and structure of cyanovinylidene complexes

Both donor or acceptor substituted aryl acetylide complexes Ru(C≡CC_6H_4R-4)(dppe)Cp (R = OMe (**3**), Me (**2**), H (**1**), CN (**4**), CO_2Me (**5**)) and the heterometallic complex Ru(C≡CFc)$(PPh_3)_2$Cp (**6**, Fc = ferrocenyl) were readily cyanated by [**9**]BF_4 in a mixed CH_2Cl_2 / NCMe solvent system (Scheme 4), to give cyanovinylidene complexes [**11** - **16**]BF_4 in good to excellent yield after purification by preparative TLC and crystallisation or precipitation. The closely related iron complexes [Fe{C=C(CN)C_6H_4R-4}(dppe)Cp]BF_4 (R = H ([**17**]BF_4), Me ([**18**]BF_4) were prepared in an entirely analogous fashion from Fe(C≡CC_6H_4R-4)(dppe)Cp (**7**, **8**) and [**9**]BF_4, and isolated in ca. 50% yield. For both metal systems, reactions conducted in CH_2Cl_2 also yielded the cyanovinylidene products, but in relatively poor isolated yield (ca. 30

%). In some cases where the BF_4^- analogues proved to be troublesome to crystallise, the use of solutions of [**9**]Br prepared in situ followed by anion metathesis gave convenient access to PF_6^- salts.

Spectroscopic data for the cyanovinylidene complexes were consistent with the proposed structures. Key features include the observation of singlet resonances in the ^{31}P NMR spectra near δ_P 38 (Ru) or 90 (Fe) ppm, the high frequency / deshielded C_α resonances in the ^{13}C NMR spectra near δ_C 350 ppm characteristic of vinylidene complexes [1], with coupling to phosphorus in evidence, and the observation of both ν(C≡N) and ν(C=C) bands in the IR spectra near 2200 and 1580 cm^{-1}, respectively. These spectroscopic features were largely insensitive to the nature of the vinylidene substituent, indicating little electronic interaction between the substituent and the metal centre.

3.6 Molecular structures of cyanovinylidene complexes

The molecular structures of the ruthenium cyanovinylidene complexes [Ru{C=C(CN)Ph}$(PPh_3)_2$Cp]X ([**11**]X, X = BF_4^-, PF_6^-), [Ru{C=C(CN)C_6H_4Me-4}$(PPh_3)_2$Cp]PF_6 ([**12**]PF_6), which was prepared by reaction of **2** with [**9**]Br and subsequent anion metathesis with NH_4PF_6 [46], as the BF_4^- salt proved resistant to crystallisation, [Ru{C=C(CN)C_6H_4CN-4}$(PPh_3)_2$Cp]BF_4 ([**14**]BF_4), and [Fe{C=C(CN)C_6H_4Me-4}(dppe)Cp]BF_4 ([**18**]BF_4) were determined by single crystal X-ray diffraction. Illustrative plots of selected cations are shown in Figures 5 - 8, and the structures may be conveniently compared with those found in [Ru{C=C(Me)Ph}$(PPh_3)_2$Cp]I ([**19**]I) [28], the cyanovinylidene [Ru{C=C(CN)C_6H_4Me}(dppe)Cp*]BF_4 ([**20**]BF_4) [46], [Fe(C=C(Ph)C_6H_4OMe-

4}(dppe)Cp][BAr^F_4] ([**21**]BAr^F_4) [36] and the sterically unencumbered example [Fe(C=CBr_2)(dppe)Cp]BF_4 ([**22**]BF_4) [34] (Table 1).

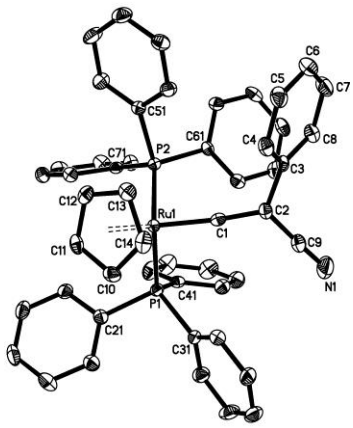

Figure 5. The structure of the cation [Ru{C=C(CN)Ph}$(PPh_3)_2$Cp]$^+$ [**11**]$^+$ showing the atom labelling scheme.

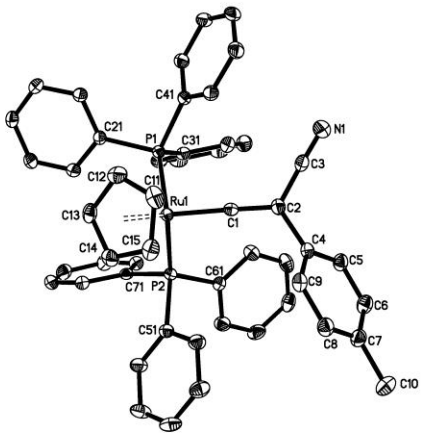

Figure 6. The structure of the cation [Ru{C=C(CN)C_6H_4Me-4}$(PPh_3)_2$Cp]$^+$ [**12**]$^+$ showing the atom labelling scheme.

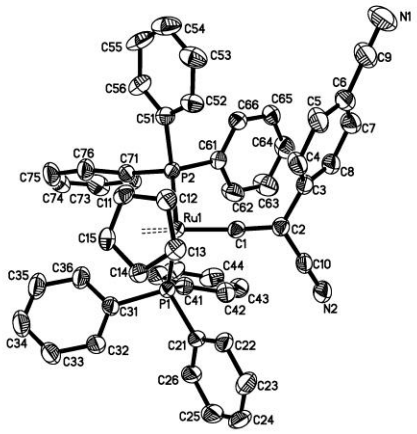

Figure 7. The structure of the cation $[Ru\{C{=}C(CN)C_6H_4CN\text{-}4\}(PPh_3)_2Cp]^+$ [**14**]$^+$ showing the atom labelling scheme.

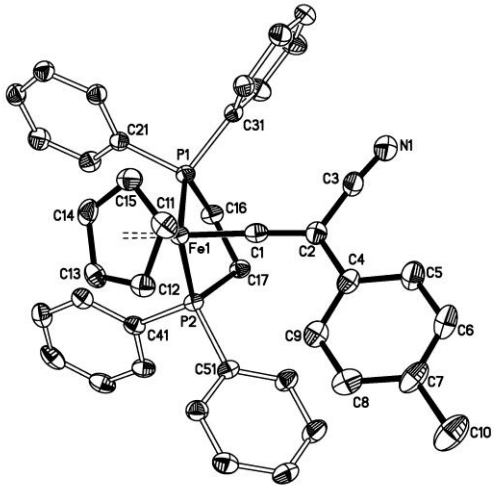

Figure 8. The structure of the cation $[Fe\{C{=}C(CN)C_6H_4Me\text{-}4\}(dppe)Cp]^+$ [**18**]$^+$ showing the atom labelling scheme.

The metal centres adopt the usual piano-stool geometry with P-M-P angles in the case of the $Ru(PPh_3)_2Cp$ based complexes being near 100° to relieve steric congestion associated with the PPh_3 ligands, but constrained to less than 90° by the ethylene bridge of the dppe ligand in the Fe(dppe)Cp and Ru(dppe)Cp* complexes contained

in Table 1. The relatively short M-C(1) and long M-P and C(1)-C(2) distances in the cyanovinylidene complexes compared with examples of the same M(PP)Cp' metal fragment featuring acetylide and vinylidene ligands are consistent with the cumulated nature of the cyanocarbon ligand, and a degree of enhanced electron-withdrawing character brought about by the presence of the cyano moiety.

There is only a very small energetic preference for vinylidene ligands coordinated to half-sandwich group 8 metals to adopt a 'horizontal' orientation, in which the plane of the vinylidene ligand lies perpendicular to the plane containing the centroid of the Cp ring [denoted Cp(0)], the metal centre and the vinylidene C_α [102], and in solution the barrier to ligand rotation was determined by NMR methods to be of the order of 9 kcal mol^{-1} [103, 104]. Nevertheless, crystallographically determined structures of $M(C_\alpha{=}C_\beta R_2)(PP)Cp'$ (M = Fe, Ru, Os) usually exhibit ligand orientations that conform to the general 'horizontal' orientation. For example, the Cp(0)-M…C_β-R angles in [**19**]$^+$, [**20**]$^+$ and [**21**]$^+$ are 116.6 / –68.2, 105.7 / –63.7 and 70.1 / –103.8°, respectively, whilst in the least sterically congested example [**22**]$^+$ the Cp(0)-M…C_β-Br angle falls closer the idealised horizontal geometry (93.72° / –88.98°). The Cp(0)-M…C(2)-CN angles in the cyanovinylidene complexes are 123.2_3 / 125.0_3 ([**11**]PF_6 / [**11**]BF_4), 102.6_6 ([**12**]PF_6), 110.8_7 and 120.2_6 (two independent molecules [**14**]BF_4) and -117.9_6 ([**18**]BF_4). The plane of the vinylidene is tilted from horizontal in such a way that the cyano substituent is situated away from the Cp ligand and falls into a pocket formed by the phenyl rings of the phosphine ligand(s), whilst the aromatic substituent of the vinylidene ligand is oriented in such a way as to reduce the steric congestion.

Table 1. Selected bond lengths (Å) and angles for complexes **3**, **5**, [**11**]PF_6, [**11**]BF_4, [**12**]PF_6, [**14**]BF_4, [**18**]BF_4 and related species.

	M-P(1)	M-P(2)	M-C(1)	C(1)-C(2)	C(2)-C_{Ar}	P(1)-M-P(2)	M-C(1)-C(2)	C(1)-C(2)-C_{Ar}	C(1)-C(2)-C_N
Ru(C≡CPh)(PPh_3)$_2$Cp [28, 72]	2.303 / 2.229(3)	2.285 / 2.228(3)	2.016(3) / 2.017(5)	1.215(4) / 1.214(7)	1.456(4) / 1.462(8)		178.0(2) / 177.7(4)	171.9(3) / 170.6(5)	
Ru(C≡CC_6H_4OMe)(PPh_3)$_2$Cp	2.2922(6)	2.2902(5)	2.019(2)	1.212(3)	1.442(3)	99.18(2)	176.38(18)	172.3(2)	
Ru(C≡CC_6H_4CN)(PPh_3)$_2$Cp [42]	2.3134(5)	2.3031(5)	2.011(2)	1.219(3)	1.432(3)		175.4(2)	175.1(2)	
Ru(C≡C$C_6H_4CO_2$Me)(PPh_3)$_2$Cp	2.3090(10)	2.2842(10)	2.015(4)	1.199(6)	1.441(5)	99.81(3)	175.6(4)	172.5(5)	
[Ru{C=C(CN)Ph}(PPh_3)$_2$Cp]PF_6	2.3797(7)	2.3547(6)	1.812(2)	1.344(3)	1.495(3)	101.12(2)	173.1(2)	119.4(2)	119.3(2)
[Ru{C=C(CN)Ph}(PPh_3)$_2$Cp]BF_4	2.3756(9)	2.3452(9)	1.811(4)	1.338(5)	1.494(5)	100.55(3)	173.3(3)	120.0(3)	119.3(3)
[Ru{C=C(CN)C_6H_4Me}(PPh_3)$_2$Cp]PF_6	2.3497(4)	2.3756(4)	1.8186(16)	1.341(2)	1.494(2)	100.60(2)	174.13(14)	120.65(15)	120.24(15)
[Ru{C=C(CN)C_6H_4CN}(PPh_3)$_2$Cp]BF_4	2.3706(10)	2.3613(10)	1.808(4)	1.341(5)	1.487(4)	102.04(4)	175.0(3)	119.5(3)	120.9(3)
[Ru{C=C(Me)Ph}(PPh_3)$_2$Cp]I [28]	2.341(3)	2.363(3)	1.863(10)	1.293(15)	1.477(16)	99.6(1)	172.8(11)	117.0(11)	125.1(12)[a]
[Ru{C≡C(CN)C_6H_4Me}(dppe)Cp*]BF_4	2.3260(3)	2.3140(3)	1.8134(13)	1.3343(17)	1.4904(18)	81.62(1)	171.49(11)	122.60(12)	117.06(12)
Fe(C≡CC_6H_4Me)(dppe)Cp [41]	2.1687(6)	2.1714(7)	1.9068(17)	1.220(2)	1.439(2)	85.95(2)	174.93(15)	174.84(17)	
[Fe{C≡C(CN)C_6H_4Me}(dppe)Cp]BF_4	2.2420(6)	2.1991(6)	1.722(2)	1.347(3)	1.491(3)	84.70(2)	173.76(18)	123.4(2)	119.6(2)
[Fe{C=C(Ph)C_6H_4OMe}(dppe)Cp]BAr^F_4	2.1927(8)	2.2112(9)	1.759(4)	1.310(5)	1.486(5)	85.46(3)	174.7(2)	124.4(2)	118.8(3)[b]
[Fe(C=CBr_2)(dppe)Cp]BF_4 [34]	2.2229(14)	2.2164(14)	1.823(6)	1.192(8)	1.923(6)[c]	84.30(5)	179.1(5)	122.9(5)	125.3(5)
[Fe{C=C(CN)C_6H_4Me}(dppe)Cp]BF_4	2.2420(6)	2.1991(6)	1.722(2)	1.347(3)	1.491(3)	84.70(2)	173.76(18)	123.4(2)	119.6(2)

[a] C(1)-C(2)-Me [b] C(1)-C(2)-C_{ArOMe} [c] C(2)-Br

3.7 Electrochemistry

The electrochemical response of ruthenium(II) acetylide complexes of general form Ru(C≡CAr)(PP)Cp' (Ar = aromatic substituent, PP = phosphine donors, Cp' = Cp, Cp*) is characterised by an oxidation event that has considerable ethynyl ligand character, and as such the potentials of these redox processes, and the chemical stability of the resulting radical cations, is sensitive to the nature of the aromatic group and the electronic properties of substituents [40, 81]. However, the different combinations of solvent, supporting electrolyte, temperature and reference electrode employed in collecting the range of available data can make direct comparisons of the results collated from many different research groups difficult, especially in the absence of a reported potential for an internal reference compound [105]. Table 2 summarises the redox behaviour of a number of acetylide complexes pertinent to the present study in CH_2Cl_2 / 0.1 M NBu_4BF_4, reported on the SCE reference scale through correction against an internal ferrocene or decamethylferrocene couple ($FeCp_2$ / $[FeCp_2]^+$ = 0.45 V; $FeCp^*_2$ / $[FeCp^*_2]^+$ = –0.07 V).

The cyclic voltammogram (ν = 100 mV / s) of the parent compound $Ru(C{\equiv}CPh)(PPh_3)_2Cp$ (**1**) exhibits an oxidation wave at +0.54 V, which is only partially chemically reversible, even at –40°C [40], as a result of the redox non-innocent nature of the phenylethynyl ligand and rapid dimerisation of the largely ligand-based radical cation in solution [106]. A completely irreversible wave is also observed at higher potentials (+1.34 V). On the timescale of the CV experiment, the electrochemically generated tolyl derivative $[Ru(C{\equiv}CC_6H_4Me\text{-}4)(PPh_3)_2Cp]^+$ ($[\mathbf{2}]^+$) is more stable, and the first electrochemical oxidation becomes chemically reversible. The electrochemical behaviour of other complexes $[Ru(C{\equiv}CC_6H_4R\text{-}4)(PPh_3)_2Cp]$ is

similar, with $E_{1/2}$ values following predictable trends so that electron donating groups (R = OMe (**3**)) result in a cathodic shift in both redox processes, while electron withdrawing groups (R = CN (**4**), CO_2Me (**5**)) cause anodic shifts. In each case, the chemical reversibility improved at lower temperatures, although the slower diffusion and increased solution resistance at low temperatures resulted in more sluggish electron transfer processes, and larger ΔE_p values. The electrochemical response of the ferrocene derivative $Ru(C{\equiv}CFc)(PPh_3)_2Cp$ (**6**) is characterised by a ferrocene based oxidation at +0.12 V, with the resulting ferrocenium cation cathodically shifting the metal-ethynyl based oxidation to +0.81 V [43]. The iron complexes $Fe(C{\equiv}CC_6H_4R\text{-}4)(dppe)Cp$ (R = H (**7**), Me (**8**)) exhibit a more chemically reversible one-electron oxidation wave at modest electrode potentials in the cyclic voltammograms. These oxidation processes are some 200 mV less thermodynamically favourable than well-known and extensively investigated Cp* analogues [107]. For both supporting metal-ligand fragments ($Ru(PPh_3)_2Cp$ and Fe(dppe)Cp), the replacement of the arylethynyl ($C{\equiv}CC_6H_4R\text{-}4$) ligand by the cyanoacetylide ($C{\equiv}CC{\equiv}N$) ligand results in fully reversible redox system [89, 91], with the most anodic oxidation potentials in their respective series. The shift of the cyanoacetylide oxidation to more positive potentials relative to the aryl ethynyl systems is smaller for the iron family ($Fe(C{\equiv}CC{\equiv}N)(dppe)Cp$ ca. +250 mV relative to $Fe(C{\equiv}CC_6H_4Me\text{-}4)(dppe)Cp$) than ruthenium ($Ru(C{\equiv}CC{\equiv}N)(PPh_3)_2Cp$ ca. +530 mV relative to $Ru(C{\equiv}CC_6H_4Me\text{-}4)(PPh_3)_2Cp$), which reflects the greater metallic character in the redox active orbital of the iron systems.

The electrochemical responses of the mono- and di-cyanovinylidene complexes $[Ru\{C{=}C(CN)C_6H_4Me\text{-}4\}(dppe)Cp^*]BF_4$ and $[Ru\{C{=}C(CN)_2\}(dppe)Cp^*]BF_4$ are

each characterised by an irreversible oxidation and a quasi-reversible reduction in CH_2Cl_2 / 0.1 M NBu_4BF_4 (Table 2) [46]. Each of the ruthenium cyanovinylidene complexes [**11**]BF_4, [**12**]BF_4, [**13**]BF_4, [**14**]BF_4 and [**15**]BF_4 behaved similarly, and exhibited an irreversible oxidation, some 1.1 – 1.3 V more positive than the analogous acetylide and likely to have more metallic character, and a chemically irreversible reduction in CH_2Cl_2 / 0.1 M NBu_4BF_4 (Table 2). The reversibility of the process did not improve at lower temperatures, and the reverse waves became even less distinct, probably indicating slow back electron transfer kinetics. The peak potential of the reduction process displayed a systematic shift in line with the electronic properties of the vinylidene substituent, and whilst the oxidation potentials spanned ca. 140 mV, no systematic trends were apparent. In the case of the ferrocenyl complex [**16**]BF_4 an electrochemically reversible ferrocene-based oxidation was observed at 0.58 V which likely arise from a combination of the *gem*-cyano moiety and the complex charge, with the irreversible oxidation associated with the ruthenium centre being found at 1.91 V. A second irreversible oxidation was observed in [**13**]BF_4, and attributed to oxidation of the anisole moiety. The iron complexes [**17**]BF_4 and [**18**]BF_4 gave more chemically reversible electrochemical response, with the reduction process being reversible even at room temperature, although the oxidation events still showed signs of chemical complications. Comparing the electrochemical response of cyanovinylidenes across the series derived from $Ru(PPh_3)_2Cp$ and Fe(dppe)Cp, whilst the metal-based oxidation event in the case of iron complexes was shifted some –100 to –300 mV relative to the ruthenium analogue, the potential of the reduction event was largely insensitive to the nature of the metal, thereby supporting the chemically intuitive assignment of the reduction to a ligand centred process.

Table 2. The electrochemical response of aryl acetylide, cyanoacetylide and cyanovinylidene complexes.[a]

	Fc/Fc^{+} [b]	Fc^*/Fc^{*+} [c]	$E^o_{(1/2)}$ [d]	$i_{pa}:i_{pc}$ [e]	ΔE_p [f]	$E^r_{(1/2)}$ [g]	$i_{pc}:i_{pa}$ [h]	ΔE^r_p [i]
$[Ru(C{\equiv}CC_6H_5)(PPh_3)_2Cp]$ (–40 °C) **1** [40]		-0.07	0.54	1.7	115			
$[Ru(C{\equiv}CC_6H_4Me\text{-}4)(PPh_3)_2Cp]$ **2** [40]		-0.07	0.48	1.0	120			
$[Ru(C{\equiv}CC_6H_4OMe\text{-}4)(PPh_3)_2Cp]$ **3**		-0.07	0.38	1.3	100			
$[Ru(C{\equiv}CC_6H_4OMe\text{-}4)(PPh_3)_2Cp]$ **3** (–40 °C)		-0.07	0.41	1.0	240			
$[Ru(C{\equiv}CC_6H_4CN\text{-}4)(PPh_3)_2Cp]$ **4**		-0.07	0.64	2.2	120			
$[Ru(C{\equiv}CC_6H_4CN\text{-}4)(PPh_3)_2Cp]$ **4** (–40 °C)		-0.07	0.64	1.0	153			
$[Ru(C{\equiv}CC_6H_4CO_2Me\text{-}4)(PPh_3)_2Cp]$ **5**		-0.07	0.61 (p_a,[j] irr[k])					
$[Ru(C{\equiv}CC_6H_4CO_2Me\text{-}4)(PPh_3)_2Cp]$ **5** (–40 °C)		-0.07	0.57	1.0	83			
$[Ru(C{\equiv}CFc)(PPh_3)_2Cp]$ **6** [43]	0.45		0.12, 0.81	1.0, 1.0	80, 90			
$[Ru(C{\equiv}CCN)(PPh_3)_2Cp]$ [89]	0.45		0.91	1.0				
$[Fe(C{\equiv}CC_6H_5)(dppe)Cp]$ **7**	0.45		0.06	1.0	145			
$[Fe(C{\equiv}CC_6H_4Me\text{-}4)(dppe)Cp]$ **8**	0.45		0.04	1.0	115			
$[Fe(C{\equiv}CCN)(dppe)Cp]$ [91]	0.45		0.29	1.0				
$[Ru\{C{=}C(CN)C_6H_5\}(PPh_3)_2Cp]BF_4$ [**11**]BF_4	0.45		1.86 (p_a, irr)			-0.93 (p_a, irr)		
$[Ru\{C{=}C(CN)C_6H_4Me\text{-}4\}(PPh_3)_2Cp]BF_4$ [**12**]BF_4	0.45		1.86 (p_a, irr)			-0.93(p_a, irr)		
$[Ru\{C{=}C(CN)C_6H_4OMe\text{-}4\}(PPh_3)_2Cp]BF_4$ [**13**]BF_4	0.45		1.77 (p_a, irr)			-1.11 (p_a, irr)		
$[Ru\{C{=}C(CN)C_6H_4CN\text{-}4\}(PPh_3)_2Cp]BF_4$ [**14**]BF_4	0.45		1.72 (p_a, irr)			-0.81 (p_a, irr)		
$[Ru\{C{=}C(CN)C_6H_4CO_2Me\text{-}4\}(PPh_3)_2Cp]BF_4$ [**15**]BF_4	0.45		1.86(p_a, irr)			-0.86 (p_a, irr)		
$[Ru\{C{=}C(CN)Fc\}(PPh_3)_2Cp]BF_4$ [**16**]BF_4		-0.07	0.58	1.0	90	-1.06 (p_a, irr)		
$[Fe\{C{=}C(CN)C_6H_5\}(dppe)Cp]BF_4$ [**17**]BF_4	0.45		1.76 (p_a, irr)	3.5		-0.95	1.0	105
$[Fe\{C{=}C(CN)C_6H_4Me\text{-}4\}(dppe)Cp]BF_4$ [**18**]BF_4	0.45		1.56 (qr[l])	1.2		-0.95	1.0	115

[a] for general conditions, see the Experimental section 2.1. [b] Fc/Fc^+ = half-wave potential of an internal ferrocene standard (V). [c] Fc^*/Fc^{*+} = half-wave potential of an internal decamethylferrocene standard (V). [d] $E^o_{(1/2)}$ = half-wave potential of an oxidation wave (V). [e] $i_{pa}:i_{pc}$ = ratio of anodic to cathodic peak current for an oxidation. [f] ΔE_p = separation of anodic and cathodic peaks (V). [g] $E^r_{(1/2)}$ = half-wave potential of a reduction wave (V). [h] $i_{pc}:i_{pa}$ = ratio of cathodic to anodic peak current for a reduction. [i] ΔE^r_p = separation of cathodic and anodic peaks (V). [j] p_a = anodic peak potential. [k] irr = irreversible. [l] qr = quasi-reversible.

3.8 Electronic structure calculations and spectroelectrochemistry

To gain further insight into the nature of the electrochemically generated products a series of DFT calculations and IR spectroelectrochemical studies were undertaken. Related results from [Ru{C=C(CN)C_6H_4Me-4}(dppe)Cp*]BF_4 ([**20**]BF_4) have been communicated previously [46].

DFT calculations were carried out on both [Ru{C=C(CN)Ph}$(PPh_3)_2$Cp]$^+$ (denoted [**11'**]$^+$ to distinguish the experimental and model systems) and [Fe{C=C(CN)Ph}(dppe)Cp]$^+$ ([**17'**]$^+$), using the crystallographically determined structures of [**11**]BF_4 and [**18**]BF_4 as starting points for further geometry optimisation. As a trade-off against the larger ligand sets, the relatively small 3-21G* basis set was employed with the B3LYP functional, although it should be noted that the 3-21G* basis set has proven to be sufficient to provide good agreement with experimental data in previous studies of half-sandwich ruthenium complexes [40]. The results of geometry optimisations are summarised in Table 3, and important bond lengths and angles are listed together with data from the most closely related X-ray data. The calculated bond lengths differ from those determined crystallographically by less than 0.035Å, and the optimised geometries also reproduce details of the molecular structures, such as the Cp(0)-Fe…C(2)-C_{Ar} torsion angle (56.39° [**17'**]$^+$; 55.24° [**18**]$^+$). In addition, the calculated frequencies reproduce the experimental results extremely well (Table 3). The good agreement between these data from the experimental and computational systems gives confidence in the accuracy of the computational model, and the subsequent conclusions.

Table 3. Selected bond lengths (Å), angles (°) and vibrational frequencies (cm^{-1}) from [**11**]BF_4, [**18**]BF_4 and the optimised structures (B3LYP/3-21G*) of [**11'**]$^{n+}$ and [**17'**]$^{n+}$ (n = 1, 0).

	[**11**]BF_4	[**11'**]$^+$	[**11'**]	[**18**]BF_4	[**17'**]$^+$	[**17'**]
M-P(1)	2.3756(9)	2.399	2.336	2.2420(6)	2.216	2.140
M-P(2)	2.3452(9)	2.385	2.333	2.1991(6)	2.210	2.140
M-C(1)	1.811(4)	1.840	1.960	1.722(2)	1.694	1.820
C(1)-C(2)	1.338(5)	1.330	1.352	1.347(3)	1.335	1.353
C(2)-C_{Ar}	1.4944(5)	1.509	1.496	1.491(3)	1.497	1.493
P(1)-M-P(2)	100.55(3)	102.4	102.0	84.70(2)	86.5	88.0
M-C(1)-C(2)	173.3(3)	176.4	167.3	173.76(18)	170.3	162.8
C(1)-C(2)-C_{Ar}	120.0(3)	119.2	122.9	123.4(2)	125.2	123.5
C(1)-C(2)-C_N	119.3(3)	119.9	119.9	119.6(2)	117.1	119.7
Cp(0)-M…C(2)-CN	125.03	119.9	140.5	-117.9_6	–113.0	–150.5
ν(CN)	2202	2194 [a]	[a] 2158	2203	2201 [a]	2150 [a]
ν(C=C)	1582	1594 [a]	[a] 1459	1583	1589 [a]	1457 [a]

[a] 0.95 correction factor applied

The general features of the electronic structures of [**11'**]$^+$ and [**17'**]$^+$ are similar (Figure 9), although there is some re-ordering of the orbitals associated with the vinylidene phenyl substituent with respect to the occupied orbitals from the metal fragment. As a result the phenyl group features in the HOMO–3 in [**11'**]$^+$ and the HOMO–1 in [**17'**]$^+$. In each case, the HOMO is comprised of a filled-filled interactions between a metal d-orbital and the vinylidene C=C π-system, which is also delocalised further on the phenylene substitutent in the iron derivative. Such extended delocalisation is not possible in the ruthenium example given the conformation of the

phenylene ring with respect to the plane of the vinyldene π-system. The LUMO has considerable C(1) p-orbital character, is anti-bonding in character with respect to the metal d-orbital of appropriate π-symmetry, and is approximately orthogonal to the filled orbitals that comprise the HOMO and C=C π-bond. The higher unoccupied orbitals have more metal fragment character, and if the local coordinate system is defined with *z* along the M=C=C axis and *x* and *y* directed along the M-P bonds, the LUMO+1 can be considered as the d_{x2-y2} orbital.

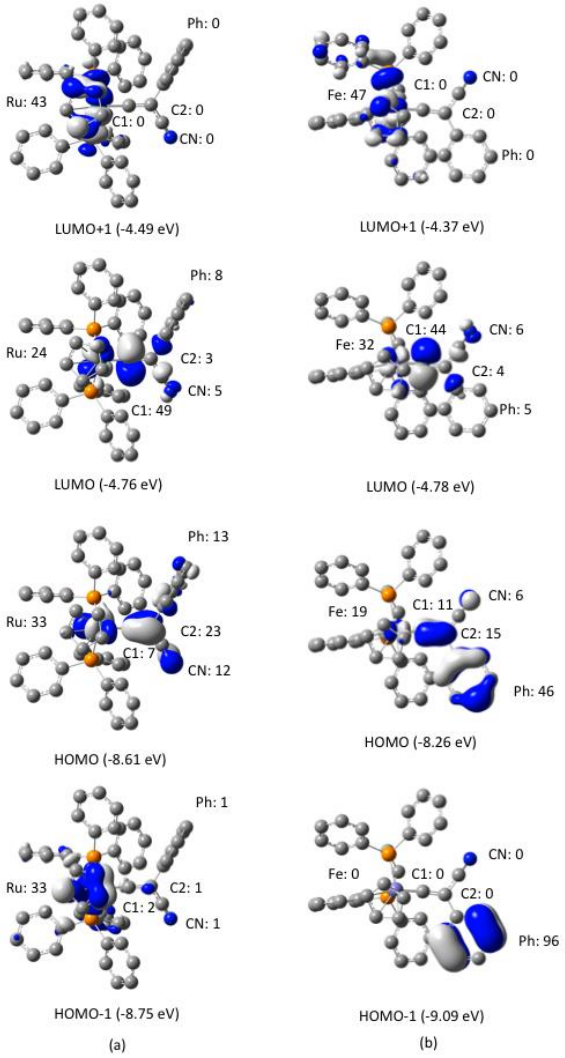

Figure 9. The energy and composition (%) of the HOMO–1 to LUMO+1 calculated for (a) [**11'**]$^+$ (b) [**17'**]$^+$ with contours plotted at ±0.04 (e/bohr^3)$^{1/2}$.

Given the more chemically reversible electrochemical reduction of the iron cyanovinylidene complexes at room temperature, complex [**18**]BF_4 was selected as a suitable candidate through which to investigate the structural effects of the redox processes by IR spectroelectrochemical methods. However, oxidation of [**18**]BF_4 proved to be chemically irreversible on the longer timescale of the spectroelectrochemical experiment, and this process was not investigated further. In contrast, despite the sluggish electron transfer behaviour observed in the voltammetry cell, [**18**]$^{\cdot}$ displayed sufficient chemical stability to be generated within the spectroelectrochemical cell, and re-oxidised to permit recovery of the closed-shell cation [**18**]$^{+}$ (Figure 10). The ν(CN) band in [**18**]$^{+}$ is observed at 2203 cm^{-1}, with the vinylidene ν(C=C) at 1583 cm^{-1}. Reduction to [**18**]$^{\cdot}$ is accompanied by a shift in the ν(CN) band by –39 cm^{-1} with an evident shoulder on the high frequency side, although the ν(C=C) cannot be observed and is likely obscured by residual bands from the supporting electrolyte. Similar behaviour has been noted for the ruthenium complexes [**20**]$^{+}$ and [**20**]$^{\cdot}$ [46]. In both cases, the limited shift of the ν(CN) band argues against reduction at the methylene carbon (C(2)). Reduction at the vinylidene alpha carbon C(1), which is consistent with the composition of the LUMO, is more in keeping with the spectroelectrochemical results.

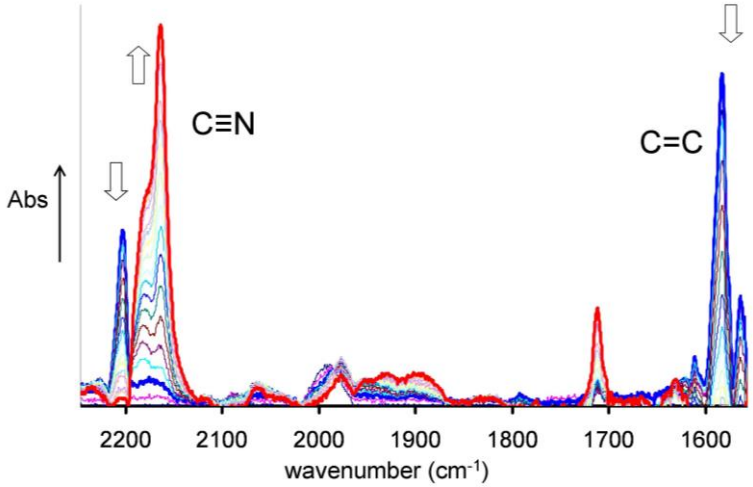

Figure 10. The IR spectra of [**18**]$^+$ and [**18**] collected in a spectroelectrochemical cell (0.1 M NBu_4BF_4 / CH_2Cl_2).

The computational model species [**11'**]· and [**17'**]· were constructed to support the observations made during the spectroelectrochemical work. Comparison of the structures of [**11'**]$^+$ with [**11'**], and of [**17'**]$^+$ with [**17'**] reveal an elongation of the M-P(1, 2) distances, consistent with an increase in electron density at the metal centre. The M-C(1) distances in the neutral radicals are some 7% longer than in the closed-shell cations, with a smaller elongation (ca. 1%) also evidence in the C(1)=C(2) distance. The M-C(1)-C(2) angle is also distorted from linearity, and taken together these metric data are consistent with an evolution from sp towards sp^2 hybridisation at C(1), and occupation of an orbital with M-C anti-bonding character. The α-HOSOs in [**11'**] and [**17'**] (Figure 11) are similar in composition to the LUMOs in [**11'**]$^+$ and [**17'**]$^+$, respectively (Figure 9). The reduced systems can therefore be represented by the simple valence descriptions shown in Figure 12.

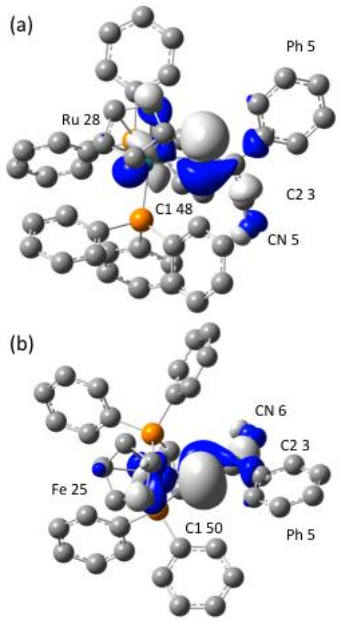

Figure 11. The α-HOSO of (a) [**11'**] (b) [**17'**], plotted with contour at ±0.04 $(e/bohr^3)^{1/2}$.

Finally, frequency calculations for each of [**11'**] and [**17'**] predict a small shift in the ν(CN) to lower frequency. Calculations on a rotational isomer of [**11'**] (Cp(0)-Fe…C(2)-C_{Ar} = 150.78°), which was also an energy minimum and essentially isoenergetic with [**11'**] being only 1 kcal mol^{-1} more stable) , gave a slightly higher ν(CN) frequency (2161 cm^{-1}). It is therefore likely that the shoulder observed in the spectroelectrochemical experiment arises from a rotational isomer of [**11'**]; the presence of such isomers is also consistent with the generally sluggish (non-diffusion controlled) electrochemical response observed in solution.

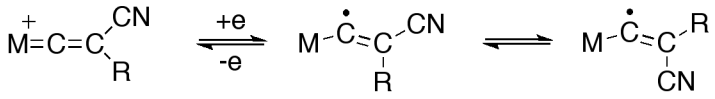

Figure 12 A simple valence bond representation of the reduction of cyanovinylidene complexes.

4. **Conclusion** A convenient synthetic route to cyanovinylidene complexes has been developed from the reactions of metal acetylide precursors with 1-cyano-4-dimethylaminopyridinium tetrafluoroborate ([**9**]BF_4). Despite the presence of the cyanomethylidene fragment, electrochemical reduction takes place at the carbene C_α carbon. Given the recent demonstrations of the facile conversion of disubstituted vinylidenes to alkynes at half-sandwich ruthenium and iron centres [37], future work from this group will address the potential to use a combination of these chemistries to provide a simple ruthenium-catalysed route to cyanoalkynes [108] from [**9**]BF_4 and terminal alkynes and to make these useful reagents readily available.

Acknowledgements We thank the EPSRC and the University of Durham for financial support. PJL holds an EPSRC Leadership Fellowship.

Supporting Information Available Tables of the energy and composition of selected frontier orbitals calculated for [**11'**]$^+$, [**11'**], [**17'**]$^+$ and [**17'**]. Crystallographic data can be obtained from the Cambridge Crystallographic Data Centre (http://www.ccdc.cam.ac.uk/), reference numbers 843000 - 843006.

References

1. M.I. Bruce, Chem. Rev. 91 (1991) 197.
2. M.I. Bruce, Chem. Rev. 98 (1998) 2797.
3. J.M. Lynam, Chem. Eur. J. 16 (2010) 8238.
4. C. Bruneau, P.H. Dixneuf, Acc. Chem. Res. 32 (1999) 311.
5. M.C. Puerta, P. Valerga, Coord. Chem. Rev. 193-195 (1999) 977.

6. A.M. Lozano-Villa, S. Monseat, A. Bajek, F. Verpoort, Chem. Rev. 110 (2010) 4865.
7. O.S. Mills, A.D. Redhouse, Chem. Commun. (1966) 444.
8. O.S. Mills, A.D. Redhouse, J. Chem. Soc. A (1968) 1282.
9. R.B. King, M.S. Saran, J. Am. Chem. Soc., 94 (1972) 1784.
10. R.B. King, M.S. Saran, J. Chem. Soc., Dalton Trans. (1972) 1053.
11. V. Cadierno, M.P. Gamasa, J. Gimeno, Eur. J. Inorg. Chem. (2001) 571.
12. J.P. Selegue, Coord. Chem. Rev. 248 (2004) 1543.
13. M.I. Bruce, Coord. Chem. Rev. 248 (2004) 1603.
14. B.M. Trost, A. McClory, Chem. Asian J. 3 (2008) 164.
15. C. Bruneau, P.H. Dixneuf, Angew. Chem. Int. Ed. 45 (2006) 2176.
16. R.B. King, Coord. Chem. Rev. 248 (2004) 1533.
17. R.B. King, M.S. Saran, J. Am. Chem. Soc. 95 (1973) 1811.
18. R.M. Kirchner, J.A. Ibers, J. Organomet. Chem. 82 (1974) 243.
19. S. Bordoni, L. Busetto, C. Camiletti, V. Zanotti, V.G. Albano, M. Monari, F. Prestopino, Organometallics 16 (1997) 1224.
20. R.B. King, M.S. Saran, J. Am. Chem. Soc. 95 (1973) 1817.
21. R.M. Kirchner, J.A. Ibers, M.S. Saran, R.B. King, J. Am. Chem. Soc. 95 (1973) 5775.
22. R.M. Kirchner, J.A. Ibers, Inorg. Chem. (1974) 1667.
23. R.B. King, M.S. Saran, D.P. McDonald, S.P. Diefenbach, J. Am. Chem. Soc. 101 (1979) 1138.
24. S. Chaona, F.J. Lalor, G. Ferguson, M.M. Hunt, J. Chem. Soc., Chem. Commun. (1988) 1606.
25. S. Abbott, S.G. Davies, P. Warner, J. Organomet. Chem. 246 (1983) C65.

26. A. Davison, J.P. Selegue, J. Am. Chem. Soc. 100 (1978) 7763.

27. M.I. Bruce, R.C. Wallis, J. Organomet. Chem. 161 (1978) C1.

28. M.I. Bruce, M.G. Humphrey, M.R. Snow, E.R.T. Tiekink, J. Organomet. Chem. 314 (1986) 213.

29. M.I. Bruce, R.C. Wallis, Aust. J. Chem. 32 (1979) 1471.

30. M.I. Bruce, C. Dean, D.N. Duffy, M.G. Humphrey, G.A. Koutsantonis, J. Organomet. Chem. 295 (1985) C40.

31. M.P. Boone, D.W. Stefan, Organometallics 30 (2011) 5537.

32. M.I. Bruce, M.G. Humphrey, G.A. Koutsantonis, B.K. Nicholson, J. Organomet. Chem. 296 (1985) C47.

33. M.I. Bruce, G.A. Koutsantonis, M.J. Liddell, B.K. Nicholson, J. Organomet. Chem. 320 (1987) 217.

34. N.J. Brown, M.A. Fox, M.E. Smith, D.S. Yufit, J.A.K. Howard, P.J. Low, J. Organomet. Chem. 694 (2009) 4042.

35. Y. Ikeda, T. Yamaguchi, K. Kanao, K. Kimura, S. Kamimura, Y. Mutoh, Y. Tanabe, Y. Ishii, J. Am. Chem. Soc. 130 (2008) 16856.

36. Y. Mutoh, Y. Ikeda, Y. Kimura, Y. Ishii, Chem. Lett. 38 (2009) 534.

37. Y. Mutoh, K. Imai, Y. Kimura, Y. Ikeda, Y. Ishii, Organometallics 30 (2011) 204.

38. M.J. Shaw, S.W. Bryant, N. Rath, Eur. J. Inorg. Chem. (2007) 3943.

39. V.K. Singh, E. Bustelo, I. de los Ríos, I. Macías-Arce, M.C. Puerta, P. Valerga, M.A. Ortuño, G. Ujaque, A. Lledós, Organometallics, 30 (2011) doi: 4014.

40. M.A. Fox, R.L. Roberts, W.M. Khairul, F. Hartl, P.J. Low, J. Organomet. Chem. 692 (2007) 3277.

41. W.M. Khairul, M.A. Fox, N.N. Zaitseva, M. Gaudio, D.S. Yufit, B.W. Skelton, A.H. White, J.A.K. Howard, M.I. Bruce, P.J. Low, Dalton Trans. (2009) 610.

42. R.L. Cordiner, D. Albesa-Jove, R.L. Roberts, J.D. Farmer, H. Puschmann, D. Corcoran, A.E. Goeta, J.A.K. Howard, P.J. Low, J. Organomet. Chem. 690 (2005) 4908.

43. M.I. Bruce, P.J. Low, F. Hartl, P.A. Humphrey, F. de Montigny, M. Jevric, C. Lapinte, G.J. Perkins, R.L. Roberts, B.W. Skelton, A.H. White, Organometallics 24 (2005) 5241.

44. M. Sata, H. Shintate, Y. Kawata, M. Sekino, M. Katada, S. Kawata, Organometallics 13 (1994) 1956.

45. C. Bitcon, M.W. Whiteley, J. Organomet. Chem. 336 (1987) 385.

46. N.J. Brown, P.K. Eckert, M.A. Fox, D.S. Yufit, J.A.K. Howard, P.J. Low, Dalton Trans. (2008) 433.

47. A. Rosiak, W. Frey, J. Christoffers, Eur. J. Org. Chem. (2006) 4044.

48. Q. Li, A.V. Rukavishnikov, P.A. Petukhov, T.O. Zaikova, C. Jin, J.F.W. Keana, J. Org. Chem. 68 (2003) 4862.

49. M. I. Bruce, C. Hameister, A.G. Swincer, R.C. Wallis, Inorg. Synth. 18 (1990) 270.

50. M.I. Bruce, C. Hameister, A.G. Swincer, R.C. Wallis, Inorg. Synth. 21 (1982) 78.

51. M. Krejcik, M. Danek, F. Hartl, J. Electroanal. Chem. 317 (1991) 179.

52. *Gaussian 09, Revision A.02*, M. J. Frisch, G. W. Trucks, H. B. Schlegel, G. E. Scuseria, M. A. Robb, J. R. Cheeseman, G. Scalmani, V. Barone, B. Mennucci, G. A. Petersson, H. Nakatsuji, M. Caricato, X. Li, H. P.

Hratchian, A. F. Izmaylov, J. Bloino, G. Zheng, J. L. Sonnenberg, M. Hada, M. Ehara, K. Toyota, R. Fukuda, J. Hasegawa, M. Ishida, T. Nakajima, Y. Honda, O. Kitao, H. Nakai, T. Vreven, J. A. Montgomery, Jr., J. E. Peralta, F. Ogliaro, M. Bearpark, J. J. Heyd, E. Brothers, K. N. Kudin, V. N. Staroverov, R. Kobayashi, J. Normand, K. Raghavachari, A. Rendell, J. C. Burant, S. S. Iyengar, J. Tomasi, M. Cossi, N. Rega, J. M. Millam, M. Klene, J. E. Knox, J. B. Cross, V. Bakken, C. Adamo, J. Jaramillo, R. Gomperts, R. E. Stratmann, O. Yazyev, A. J. Austin, R. Cammi, C. Pomelli, J. W. Ochterski, R. L. Martin, K. Morokuma, V. G. Zakrzewski, G. A. Voth, P. Salvador, J. J. Dannenberg, S. Dapprich, A. D. Daniels, O. Farkas, J. B. Foresman, J. V. Ortiz, J. Cioslowski, D. J. Fox, Gaussian, Inc., Wallingford CT, 2009.

53. A.D. Becke, J. Chem. Phys. 98 (1993) 5648.

54. C. Lee, W. Yang, R. G. Parr, Phys. Rev. B 37 (1988) 785.

55. G. A. Petersson, M. A. Al-Laham, J. Chem. Phys. 94 (1991) 6081.

56. G. A. Petersson, A. Bennett, T. G. Tensfeldt, M. A. Al-Laham, W. A. Shirley, J. Mantzaris, J. Chem. Phys. 89 (1988) 2193.

57. A.P. Scott, L. Radom, J. Phys. Chem. 100 (1996) 16502.

58. J.C. Roder, F. Meyer, I. Hyla-Kryspin, R.F. Winter, E. Kaifer, Chem. Eur. J. 9 (2003) 2636.

59. R.D. Dennington II, T.A. Kieth, J.M. Millam, Gaussian Inc, Wallingford, CT, 2008.

60. N. M. O'Boyle, A. L. Tenderholt, K. M. Langner, J. Comp. Chem. 29 (2008) 839.

61. M.J. Mays, P.L. Sears, J. Chem. Soc., Dalton Trans. (1973) 1873.

62. G.M. Sheldrick, Acta Cryst. A64 (2008) 112.

63. O.V. Dolomanov, L.J. Bourhis, R.J. Gildea, J.A.K. Howard, H. Puschmann, J. Appl. Cryst. 42 (2009) 339.

64. C.E. Powell, M.P. Cifuentes, A.M. McDonagh, S.K. Hurst, N.T. Lucas, C.D Delfs, R. Stranger, M.G. Humphrey, S. Houbrechts, I. Asselberghs, A. Persoons, D.C.R. Hockless, Inorg. Chim. Acta 352 (2003) 9.

65. M.H. Garcia, M.P. Robalo, A.R. Dias, M.T. Duarte, W. Wenseleers, G. Aerts, E. Goovaerts, M.P. Cifuentes, S. Hurst, M.G. Humphrey, M. Samoc, B. Luther-Davies, Organometallics 21 (2002) 2107.

66. M.H. Garcia, M.P. Robalo, A.R. Dias, M.F.M. Piedade, A. Galvão, W. Wenseleers, E. Goovaerts, J. Organomet. Chem. 619 (2001) 252.

67. C.J. McAdam, A.R. Manning, B.H. Robinson, J. Simpson, Inorg. Chim. Acta 358 (2005) 1673.

68. J.A. van Rijn, E. Gouré, M.A. Siegler, A.L. Spek, E. Drent, J. Organomet. Chem. 696 (2011) 1899.

69. S. Nakanishi, K. Goda, S. Uchiyama, Y. Otsuji, Bull. Chem. Soc. Japan 65 (1992) 2560.

70. L. Medei, L. Orian, O.V. Semeikin, M.G. Peterleitner, N.A. Ustynyuk, S. Santi, C. Durante, A. Ricci, C. Lo Sterzo, Eur. J. Inorg. Chem. (2006) 2582.

71. C. Ornelas, J. Ruiz, D. Astruc, J. Organomet. Chem. 694 (2009) 1219.

72. J.M. Wisner, T.J. Bartczak, J.A. Ibers, Inorg. Chim. Acta 100 (1985) 115.

73. I.-Y. Wu, J.T. Lin, Y.S. Wen, Organometallics 18 (1999) 320.

74. I.-Y. Wu, J.T. Lin, J. Luo, C.-S. Li, C. Tsai, Y.S. Wen, C.-C. Hsu, F.-F. Yeh, S. Liou, Organometallics 17 (1998) 2188.

75. M.I. Bruce, B.C. Hall, B.D. Kelly, P.J. Low, B.W. Skelton, A.H. White, J. Chem. Soc., Dalton Trans. (1999) 3719.

76. T.J. Snaith, P.J. Low, R. Rousseau, H. Pushmann, J.A.K. Howard, J. Chem. Soc., Dalton Trans. (2001) 292.

77. I.R. Whittall, M.P. Cifuentes, M.G. Humphrey, B. Luther-Davies, M. Samoc, S. Houbrechts, A. Persoons, G.A. Heath, D.C.R. Hockless, J. Organomet. Chem. 549 (1997) 127.

78. I.R. Whittall, M.G. Humphrey, A. Persoons, S. Houbrechts, Organometallics 15 (1996) 1935.

79. I.R. Whittall, M.G. Humphrey, D.C.R. Hockless, B.W. Skelton, A.H. White, Organometallics 14 (1995) 3970.

80. A.M. McDonagh, M.P. Cifuentes, N.T. Lucas, M.G. Humphrey, S. Houbrechts, A. Persoons, J. Organomet. Chem. 605 (2000) 184.

81. F. Paul, B.G. Ellis, M.I. Bruce, L. Toupet, T. Roisnel, K. Costuas, J.-F. Halet, C. Lapinte, Organometallics 25 (2006) 649.

82. K.J. Rutan, F.J. Heldrich, L.F. Borges, J. Org. Chem. 60 (1995) 2948.

83. A.M. von Leusen, J.C. Jaget, Tetrahedron Lett. 11 (1970) 967.

84. L. Klement, K. Lennich, C.E. Tucker, P. Knockel, Tetrahedron Lett. 34 (1993) 4623.

85. *Hetero Diels-Alder Methodology in Organic Synthesis*, D.L. Boger, S.M. Weinreb, Organic Chemistry Monographs; Vol. 47, Academic Press, San Diego (1987).

86. A.I. Meyers, in *The chemistry of the cyano group*, S. Patai, Z. Rappoport (Eds) Interscience, London (1970) 356.

87. D. Martin, M. Bauer, Org. Synth. 1983, **61**, 35.

88. R.E. Murray, G. Zweifel, Synthesis 1980, 150.

89. R.L. Cordiner, D. Corcoran, D.S. Yufit, A.E. Goeta, J.A.K. Howard, P.J. Low, Dalton Trans. (2003) 3541.

90. R.L. Cordiner, M.E. Smith, A.S. Batsanov, D. Albesa-Jové, F. Hartl, J.A.K. Howard, P.J. Low, Inorg. Chim. Acta 359 (2006) 946.

91. M.E. Smith, R.L. Cordiner, D. Albesa-Jové, D.S. Yufit, F. Hartl, J.A.K. Howard, P.J. Low, Can. J. Chem. 84 (2006) 1.

92. J.P. Hitten, J.R. McCarthy, D.P. Matthews, Synthesis (1988) 470.

93. M. Wakselman, E. Guibé-Jampel, A. Raoult, W.D. Busse, J. Chem. Soc., Chem. Commun. (1976) 21.

94. J. Wu, J.T. Watson, Anal. Biochem. 258 (1998) 268.

95. U. Ohms, H. Guth, Z. Kristallogr. 166 (1984) 213.

96. Z. Dega-Szafran, M. Gdaniec, M. Grundwald-Wyspiamska, Z. Kosturkiewicz, J. Koput, P. Krzyzanowski, M. Szafran, J. Mol. Struct. 270 (1992) 99.

97. G.L. Bryant Jnr, J.A. King Jnr, Acta Crystallogr. Sect. C: Cryst. Struct. Commun. 48 (1992) 2036.

98. R. Mayr-Stein, M. Bolte, Acta Crystallogr., Sect. C: Cryst. Struct. Commun. 56 (2000) e19.

99. R.M. Mustaqim, S. Ali, I.A. Razak, H.-K. Fun, S. Goswami, A. Adak, Acta Crystallogr., Sect. E: Struct. Rep. Online 61 (2005) o3733.

100. M. Chao, E. Schempp, R.D. Rosenstein, Acta Crystallogr., Sect. B: Struct. Crystallogr. Cryst. Chem. 33 (1977) 1820.

101. S. Haddad, A. Vij, R.D. Willett, J. Chem. Cryst. 33 (2003) 245.

102. N.M. Kostic, R.F. Fenske, Organoemtallics 1 (1982) 974.

103. G. Consiglio, F. Bangerter, C. Darpin, F. Morandini, V. Lucchini, Organometallics 3 (1984) 1446.

104. G. Consiglio, F. Morandini, Inorg. Chim. Acta 127 (1987) 79.

105. N.G. Connelly, W.E. Geiger, Chem. Rev. 96 (1996) 877.

106. M.I. Bruce, A. Burgun, F. Gendron, G. Grelaud, J.F. Halet, B.W. Skelton, Organometallics 30 (2011) 2861.

107. R. Denis, L. Toupet, F. Paul, C. Lapinte, Organometallics 19 (2000) 4240.

108. H. Hopf, B. Witulski, Pure App. Chem. 65 (1993) 47.